EXHIBIT 3.13

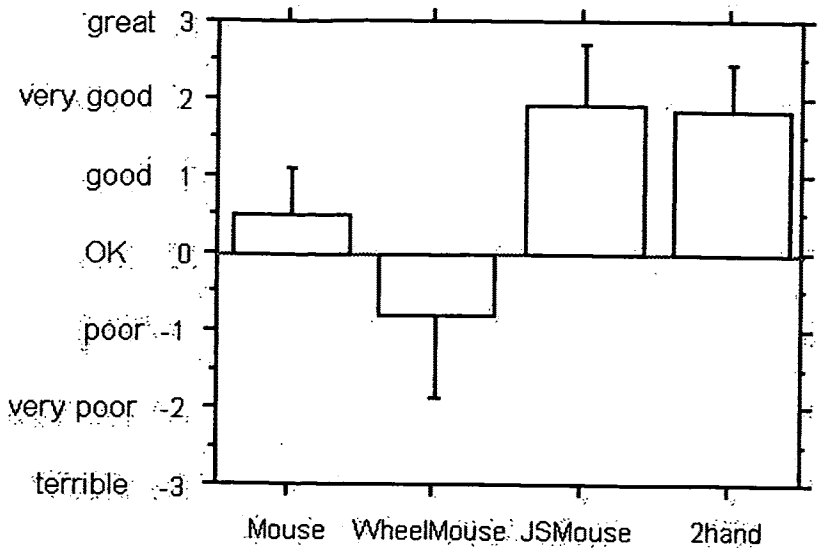

Fig. 5 Mean subjective ratings with 95% confidence error bars

Subjective ratings were similar to the performance measurements (Fig. 5), except that the difference between Mouse and WheelMouse conditions was significant: the WheelMosue received *lower* ratings than the standard mouse.

Discussions and Conclusions

JSMouse. This device outperformed the standard single stream input by a large magnitude. The isometric joystick in this design is believed to be particularly suitable for scrolling, which requires the user to control not only the final displacement of the document, but also the *speed* of the movement so that he can comfortably scan the document. As shown in our previous studies [4], position control is better conducted with isotonic devices, such as the mouse; and rate control is better conducted with isometric or elastic devices. The key factor to this compatibility is the self-centering effect in isometric or elastic devices. With self centering, rate control can be easily done. Without it, rate control requires conscious effort.

WheelMouse. Although it offered dual-stream input, the WheelMouse did not outperform the conventional single stream mouse. Some subjects commented that it was tedious and tiring to repeatedly roll the wheel, although this was an intuitive mode. The IntelliMouseTM had two additional modes: press (the wheel) and move (the mouse) and click and move, both turned the mouse into rate control mode for scrolling. Although they explored all three modes in the practice phase, only 6 subjects used the two additional rate control modes in the real tests. The lack of self-centering in the isotonic device (mouse) makes it difficult to do effective rate control.

2Hand. Interestingly, no significant performance or rating difference was found between the two handed system and the single handed JSMouse. Nonetheless, the results showed that an asymmetric two handed design, one hand with isometric rate control and the other hand with an isotonic position control, which has not been studied in the literature [e.g. 3], worked well. Questions have been raised whether such a two handed system would work at all, and whether the user would confuse the functions of the two hands. Clearly this was not the case. For more demanding tasks, we have observed more advantage with using two hands. It is extremely difficult, if not impossible, to use the one handed solutions in tasks that require parallel actions, such as scaling, translating, and rotating a 2D geometry object by controlling two vertices.

To conclude, this study indicates that it is time to add multi-stream input into mainstream commercial systems. But, each step of a new design has to be guided by thorough human factors research to avoid very possible mistakes. Further details of this study can be found in [5].

Acknowledgment

Contributions to this study were also made by Bobby Lee, Kim May, Ron Barber and Bob Olyha.

REFERENCES

[1] Buxton, W. (1986) There is more to interaction than meets the eye: some issues in manual input, in Norman, D.A and Draper, S.W. (Eds) *User Centered System Design*, Lawrence Erlbaum Associates, 319-337.

[2] Buxton, W. and Myers, B. (1986) A study of two-handed input, in *Proc. of CHI86*, 321-326.

[3] Kabbash, P., Buxton, W., Sellen, A. (1994) Two-handed input in a compound task, in *Proc. of CHI94*, 417-423.

[4] Zhai, S. (1995) *Human Performance in Six Degree of Freedom Input Control*, Ph.D. Thesis, U. Toronto. http://vered.rose.toronto.edu/people/shumin_dir/publications.html

[5] Zhai, S., Smith, B.A., Selker, T., Improving browsing performance: a study of four techniques for scrolling and pointing tasks, IBM Research Report RJ10058, Oct, 1996.

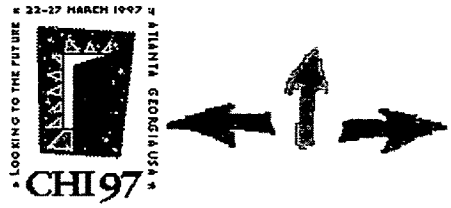

CHI 97 Electronic Publications: Late-Breaking/Short Talks

Applying Electric Field Sensing to Human-Computer Interfaces

Thomas G. Zimmerman, Joshua R. Smith, Joseph A. Paradiso, David Allport[1], Neil Gershenfeld

MIT Media Laboratory - Physics and Media Group
20 Ames Street E15-487
Cambridge, Mass 02176-4307
(617) 253-0620
tz,jrs,joep,dea,neilg @media.mit.edu

ABSTRACT

A non-contact sensor based on the interaction of a person with electric fields for human-computer interface is investigated. Two sensing modes are explored: an external electric field shunted to ground through a human body, and an external electric field transmitted through a human body to stationary receivers. The sensors are low power (milliwatts), high resolution (millimeter) low cost (a few dollars per channel), have low latency (millisecond), high update rate (1 kHz), high immunity to noise (>72 dB), are not affected by clothing, surface texture or reflectivity, and can operate on length scales from microns to meters. Systems incorporating the sensors include a finger mouse, a room that knows the location of its occupant, and people-sensing furniture. Haptic feedback using passive materials is described. Also discussed are empirical and analytical approaches to transform sensor measurements into position information.

KEYWORDS: user interface, input device, gesture interface, non-contact sensing, electric field.

INTRODUCTION

Our research on electric field (EF) based human-computer interfaces (HCI) grew out of a project to instrument Yo-Yo Ma's cello [8]. We needed to measure bow position in two axes with minimum impact on the instrument and its playability. In this paper we discuss two types of EF sensing mechanisms: *shunting*, where an external EF is effectively grounded by a person in the field; and *transmitting*, where low frequency energy is coupled into a person, making the entire body an EF emitter. The benefits of each sensing mechanism are presented along with comparisons to other sensing means. We report on several EF systems and applications, designed by arranging the size and location of EF transmitters and receivers, and suggest some future applications.

1. Visiting scientist from HP Labs, Bristol, England.

TO BE PUBLISHED IN (IEEE SIG) CHI MAY 1995

Since electric fields pass through non-conductors, passive materials that apply force and viscous friction may be incorporated into EF sensing devices, providing haptic feedback. We have constructed a pressure pad and a viscous 3-D workspace based on this principle.

PREVIOUS WORK

The first well-known use of EF sensing for human-machine interface was Leon Theremin's musical instrument. Two omnidirectional antennas were used to control the pitch and amplitude of an oscillator. Body capacitance detunes a resonant tank circuit [7]. The effect of body capacitance on electric circuits was well known to radio's pioneers, who saw the effect as an annoyance rather than an asset.

As the need for electronic security and surveillance increases, there is growing use of remote (non-contact) occupancy and motion detectors. Sensing mechanisms include capacitance, acoustic, optoelectronic, microwave, ultrasonic, video, laser, and triboelectric (detecting static electric charge) [5]. Many of these mechanisms have been adapted to measure the location of body parts in three dimensions, motivated by military cockpit and virtual reality (VR) applications [15].

Acoustic methods are line-of-sight and are affected by echoes, multi-paths, air currents, temperature, and humidity. Optical systems are also line-of-sight, require controlled lighting, are saturated by bright lights, and can be confused by shadows. Infrared systems require significant power to cover large areas. Systems based on reflection are affected by surface texture, reflectivity, and incidence angle of the detected object. Video has a slow update rate (e.g., 60 Hz) and produces copious amounts of data that must be acquired, stored, and processed. Microwaves pose potential health and regulation problems. Simple pyroelectric systems have very slow response times (>100 msec) and can only respond to changing signals. Lasers must be scanned, can cause eye damage, and are line-of-sight. Triboelectric sensing requires the detected object to be electrically charged.

Mathews [14] developed an electronic drum that detects the 3-D location of a hand-held transmitting baton relative to a planar array of antennas by using near-field signal-strength measurements. Lee, Buxton, and Smith [13] use capacitance measurement to detect multiple contacts on a touch-sensitive tablet. Both systems require the user to touch something.

Capacitive sensors can measure proximity without contact. To assist robots to navigate and avoid injuring humans, NASA has developed a capacitive reflector sensor [22] that can detects objects up to 30 cm away. The sensor uses a driven shield to push EF lines away from grounding surfaces and towards the object. Wall stud finders use differential capacitance measurement to locate wood behind plaster boards by sensing dielectric changes [6]. Linear capacitive reactance sensors are used in industry to measure the proximity of grounded objects with an accuracy of 5 microns [4]. Electrical impedance tomography places electrode arrays on the body to form images of tissue and organs based on internal electric conductivity [21].

Weakly electric fish (e.g., Gymnotiformes, sharks, and catfish) are very sophisticated users of electric fields [1]. These fish use amplitude modulation and spectral changes to determine object size, shape, conductivity, distance, and velocity. They use electric fields for social communication, identifying sex, age, and dominance hierarchy. They perform jamming avoidance when they detect the beating of their field with an approaching fish: the fish with the lower transmit frequency decreases its frequency, and the fish with the higher frequency raises its frequency. Some saltwater weakly electric fish have adapted their sensing ability to detect EF gradients as low as 5nV/cm.

Given this long history of capacitive measurement, one might wonder why EF sensing is not common in human-computer interfaces. But it is only recently that inexpensive electronic components have become available to measure the small signals produced by EF sensors. Also non-uniform electric fields have made it difficult to transform these signals into linear position coordinates. Our research addresses these issues to help make EF sensing more accessible to interface designers. It will be shown that EF sensors provide ample resolution and that converting the EF signal strength into position is the more challenging task.

MODES OF OPERATION

The Human Shunt

An electrical potential (voltage) is created between an oscillator electrode and a virtual ground electrode (Figure 1). A virtual ground is an electrical connection kept at zero potential by an operational amplifier, allowing current I_R to ground to be measured. The potential difference induces charge on the electrodes, creating an electric field between the electrodes. If the area of the electrodes is small relative to the spacing between them, the electrodes can be modeled as point charges producing dipole fields. The dipole field strength varies inversely with distance cubed. In practice the measurable field strength extends approximately two dipole lengths (distance between the transmitter and receiver electrodes). As the electrodes are moved farther apart, a larger electrode area is required to compensate for the decrease in signal strength.

When a hand, or other body part, is placed in an electric field the amount of displacement current I_R reaching the receiver decreases. This may seem counter-intuitive since the conductive and dielectric properties of the hand should increase the displacement current. However, if an object is much larger than the dipole length, the portion of the object out of the field serves as a charge reservoir, which is what we mean by "ground". The hand intercepts electric field lines, shunting them to ground, decreasing the amount of displacement current I_R reaching the receiver.

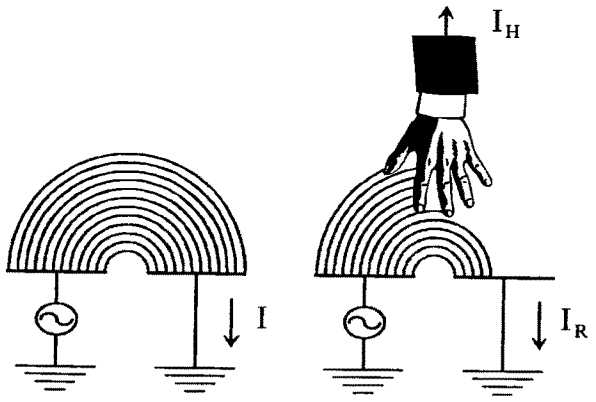

Figure 1. An electric dipole field created between an oscillating transmit electrode and virtual ground receiver electrode is intercepted by a hand. Displacement current to ground I_R decreases as the hand moves further into the dipole field.

The Human Transmitter

Low frequency energy is capacitively coupled into a person's body, making the entire person an EF emitter (Figure 2). The person can stand on, sit on, touch, or otherwise be near the oscillator electrode. One or more receiver electrodes are placed about the person. The displacement current into a receiver I_R increases as the person moves closer to that receiver. At close proximity,

the person and the receiver electrode are modeled as ideal flat plates, where displacement current varies with the reciprocal of distance. At large distances, the person and the receiver electrode are modeled as points, where displacement current varies with the reciprocal of distance squared.

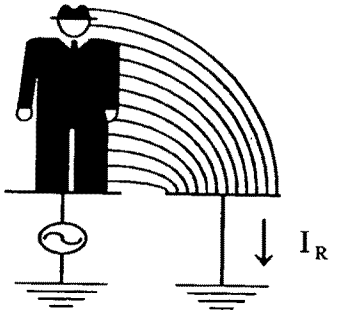

Figure 2. Energy from an oscillator is coupled into a person standing on the transmit electrode making the person an electric field emitter. As the person moves any body part closer to the grounded receive electrode, the displacement current into the receiver I_R increases.

Mode Crossover

When a hand (or any large object relative to the dipole length) approaches the dipole field of Figure 1 (shunt mode), the displacement current I_R decreases. When the hand gets very close (much less than a dipole spacing) the displacement current I_R begins to increase; the system changes from shunt mode to transmit mode. Actually both modes occur simultaneously, the hand is always coupling some field to the receiver (transmit mode) but until the hand is very close to the electrodes, the amount of displacement current shunted away from the receiver exceeds the amount coupled into the receiver.

SYSTEM HARDWARE

Signal Detection Strategy

Many capacitance detection schemes [5, 6, 13] measure the charging time of a resistor-capacitor (RC) network. The capacitance and displacement currents for EF sensing are on the order of picofarads (10^{-12} farad) and nanoamps (10^{-9} amps), requiring more sophisticated detection strategies. A synchronous detection circuit (Figure 3) is used to detect the transmitted frequency and reject all others [10], acting as a very narrow band-pass filter. Other detection methods include frequency-modulation chirps (as used in radar), frequency hopping, and code modulation (e.g., spread spectrum).

The displacement current can be measured with approximately 12 bits accuracy (72 dB) using the components shown in Figure 3. There is a trade-off between update rate (sample rate/number of samples averaged) and accuracy (signal-to-noise ratio). The signal-to-noise ratio increases as the square root of the number of samples averaged. For example, averaging 64 samples increases the signal-to-noise a factor of eight (+18 dB), with a corresponding 1/64 update rate.

Information can be coded in the modulated transmitter signal. A multitude of small EF sensing devices can be scattered about a room, like eels in a murky pond, transmitting measurements to neighboring devices with the same EF used to measure proximity. The jamming avoidance mechanism of weakly electric fish [1] suggests that such devices can adjust their transmission frequencies autonomously when new devices are introduced into the sensing space.

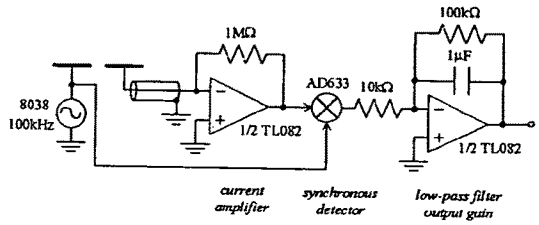

Figure 3. Synchronous detection circuitry.

Small displacement currents require good shielding, however the capacitance of shielded coaxial cable is orders of magnitude greater that the capacitance between electrodes. Cable capacitance low-pass filters the received signal, typically limiting the operating frequency to 30 kHz, and introduces a phase shift that is compensated for in the synchronous detector (not shown). Placing the current amplifier at the receiver electrode allows higher frequencies, limited by the amplifier's slew rate. For example, attaching the receive electrode directly to the TL082 current amplifier allows an operating frequency of 220 kHz.

Transmitter Power

The frequency range we use for EF HCI is 10 kHz to 200 kHz. Below this range, displacement currents and update rates are too small. Above this range FCC power regulations become more stringent [3]. The distance between electrodes is a fraction of a wavelength, so no appreciable energy is radiated. The only power consumed by the transmitter is the energy required to charge the capacitance of the transmitter electrode to the oscillating voltage.

In practice the transmitter power is less than a milliwatt. This allows the design of very low power systems with no radio interference. By adding an inductor, the transmitter can be driven into resonance, decreasing energy dissipation and increasing the transmitter potential, for example 60 volts from a 5 volt supply. A larger

transmitter potential increases the strength of the received signal and therefore the signal-to-noise ratio, producing greater spatial resolution. Transmit signal strength can be increased until the current amplifier is saturated.

"Fish" Evaluation Board

To assist researchers in exploring EF HCI, our group has produced a small microprocessor-based EF sensing unit, supporting one transmitter and four receivers (Figure 4). It is called a "fish" after the amazing EF abilities of weakly electric fish, and because fish can navigate three dimensions while a mouse can navigate only two. The evaluation board supports MIDI, RS-232, and RS-485 serial communication protocols. We are currently designing a "smart fish," a second generation EF evaluation board utilizing a digital signal processor to allow automatic calibration and the exploration of more complex detection strategies, such a spread spectrum. The smart fish also measures the power loading of the transmitter to disambiguate mode crossover. Transmitter loading is monotonic; the current drawn from the transmit electrode always increases as an object approaches the transmit electrode.

ELECTRIC FIELD GEOMETRY

The value returned by a sensor is unfortunately *not* directly proportional to the distance between a hand and

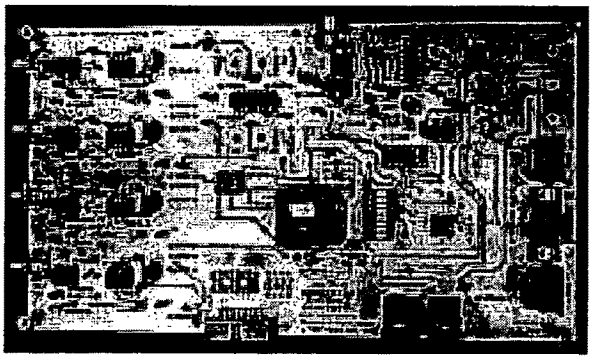

Figure 4. Fish electric field sensing evaluation board.

the sensor. Recovering information such as the *(x,y,z)* position of a hand from three sensor values *(r,s,t)* is a non-trivial problem. Solving the problem requires a model of the electric field geometry. The absolute signal strength depends on the coupling of the person to a reference (ground for shunt mode and the transmit electrode for transmit mode). This coupling acts as a global system gain. The relative signal strength of the sensors contains the position information. For this reason normalized sensor readings are used to calculate position information.

There are two basic strategies for creating this model. In the analytical approach, knowledge of electrostatics (Laplace equation) is used to derive, for a given sensor geometry, an expression for the signals received as a function of hand position. The expression is then inverted analytically or numerically. In the empirical approach, signals are measured for a variety of known hand positions, and a function (e.g., radial basis function) that converts sensor values to hand positions is fit to the resulting data set. The analytical approach provides insight into the behavior of the sensors and does not require a training phase. However, any given analytical solution is applicable only for a particular sensor geometry, and different sensor geometries require new solutions. The empirical approach is more flexible, because changes in the sensor layout or environment can be accommodated by retraining.

Since our measurements occur within a fraction of a wavelength, we are in the near-field limit where the electric field is the gradient of the potential across the electrodes, so we can treat the situation as an electrostatics problem [12]. The same physics applies for electrode spacing that ranges from microns to meters. Small electrode spacing has been used to measure position with micron resolution [19]; large electrode spacing has been used to measure the location of a person in a room. We are not interested in the absolute values of sensor values; we care only about their functional dependence on the position of the body part we are measuring. Since the human body is covered with conductive, we treat the body as a perfectly conducting object. The hand is treated as a grounded point in space. In practice, the finite area of a hand and its connection to an arm serves to blur or convolve the ideal point response. But this point approximation usually works well as long as the real hand is a constant shape, the same convolution is being applied everywhere, and so the basic functional form of the hand response will be the same as that of the point response.

In-Plane Measurements

Figure 5 shows a contour plot of the predicted received signal, calculated using the classic dipole field expression [12] for a hand moving around a *Z* plane 0.9 dipole units above the dipole axis. A dipole unit is the distance between the transmit electrode and receive electrode. The predicted contour compares well to data collected by moving a grounded cube (2.5 cm on each side) across the plane.

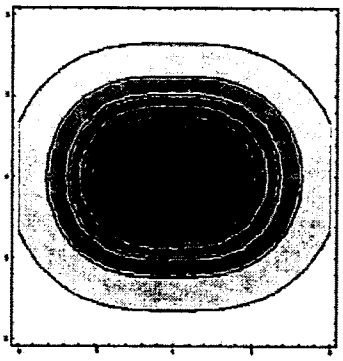

Figure 5. Contours of electric field strength in plane Z = 0.9 (measured in units of the dipole spacing) predicted by analytical model.

Out-Of-Plane Measurements

The relationship between hand proximity Z and displacement current I_R is measured using an electrical equivalent of a hand and arm suspended above the center of a dipole. The term proximity is used to emphasize that EF sensing measures the integrated (convolved) effect of an object in the electric field. When a hand is placed near a dipole, the hand, arm, and body attached to the arm all affect the field, though each contributes less as they are progressively farther away from the dipole.

The surrogate hand and arm combination is an aluminum tube 7.6 cm in diameter and 48.3 cm long and is grounded through a suspending wire for shunt mode and connected to an oscillator for transmit mode. The transmit and receiver electrode, each measuring 2.5 cm x 2.5 cm, are 15.2 cm apart on center. A least squares fit of the data reveals the following functional form for both shunt and transmit modes;

$$I_R = A + \frac{B}{\sqrt{Z}}$$

where A and B are constants determined by electrode geometry, detection circuit gain and bias, oscillator frequency and voltage, and Z is distance above the dipole. For shunt mode B is negative since displacement current I_R decreases as the object moves closer to the dipole.

Proximity resolution is expressed as the change in distance Z that produces a 6 dB change in displacement current I_R over the noise floor (two times the noise floor). The resolution is dependent on the signal-to-noise ratio of the detection system, which is a function of integration time. The longer the data is averaged, the greater the proximity resolution, albeit with a corresponding slower update rate. The fish evaluation board used in these measurements has an integration time constant of 10 milliseconds. Figure 6 plots proximity resolution as a function of distance Z for shunt mode. At 85 mm distance, proximity resolution is 1 mm.

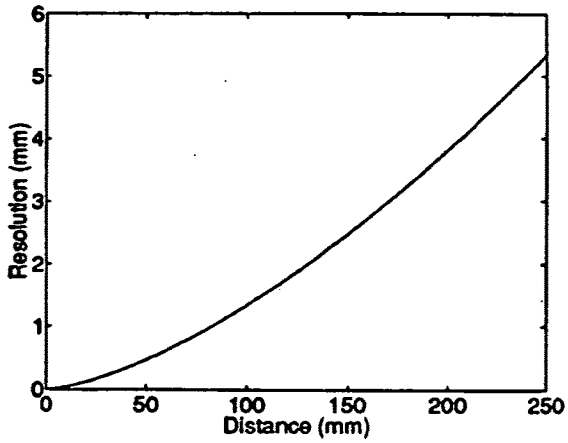

Figure 6. Proximity resolution of a surrogate arm in shunt mode plotted as a function of distance from dipole to arm. Resolution is the change in distance that produces a 6dB change in signal over noise.

Imaging: Converting Signals To Position

Each dipole measures a degree of freedom, either object position or size. A single dipole cannot distinguish a close small object from a large distant object, as both might block the same number of field lines. A second dipole operating on a longer length-scale (greater electrode spacing) can be used to distinguish these two situations, or to measure two spatial coordinates of a single fixed-size object. Three dipoles can measure the 3-D position of an object of fixed size, or determine the 2-D position and size of an object. Four dipoles can determine the size and 3-D position of an object. Five dipoles can determine the 3-D position, size, and elongation of an object. We are working on the continuum limit of adding more dipoles, to perform low-resolution imaging.

Optimal Sensor Placement

Each receiver measurement constrains the position of a small object (relative to dipole spacing) to an ellipsoid centered on the dipole axis (see Figure 5). The dipoles should be oriented orthogonally in order to minimize the sensitivity of the solution *(x,y,z)* to errors in *(r,s,t)*. The problem of inverting the sensor readings is equivalent to the geometrical problem of finding the intersection points of these ellipsoids. Often additional constraints (prior knowledge) must be imposed to select one solution from the many symmetric cases that are consistent with the data. For example, to make a two-dimensional mouse using only two dipoles, we must impose the constraint that the hand is on one side of the dipoles.

COMPARISON TO OTHER SENSOR TECHNOLOGIES

Electric field sensors detect a bulk effect, integrating the body's interception of EF. Unlike optical system, the effect does not depend on object surface texture and reflectivity. The data from EF sensors is continuous with a resolution limited by transmission strength and noise rejection. There is an economy of data; only three channels are required to locate a hand in 3-D. In comparison, a video camera produces an abundance of data, on the order of 75 megabits per second, while updating at 60 Hz. An EF system operating at 100 kHz can average 100 samples, provide a 1 kHz update rate, with 1 millisecond lag time.

Electric field systems can be extremely small, light-weight and low power, as required by the ever shrinking real estate and energy capacity of lap, palm, and watch based computers. Since electric fields penetrate non-conductors, sensors can be hidden, providing protection from weather and wear, as well as adding an element of magic to the interface.

SYSTEM CONFIGURATIONS AND APPLICATIONS

The transmit method provides large receive signals, operates over large areas, and can distinguish multiple persons. Capacitively coupling energy into a person requires continuous close contact with the person. We have used transmit electrode ranging from 5 to 150 square cm, depending on proximity to the person. The transmit electrode can be incorporated into the seat of a chair, a section of a floor, the back of a palm computer, or a wristwatch band. Direct conductive contact with the person's skin requires a much smaller electrode area (<5 square cm). Asymmetric placement of receiver electrodes helps decouple signal strength from position calculations.

The shunt method does not require close contact with a person. For each dimension, a minimum of one receiver is required. Prototyping interfaces is basically an "arts and crafts" project, consisting of cutting out electrodes, typically aluminum foil and copper tape, taping them down, and wiring them up to the fish evaluation unit.

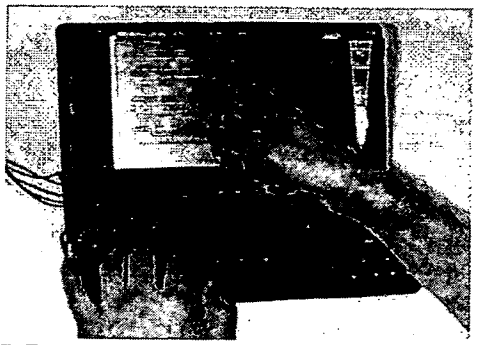

Figure 7. Two-dimensional finger-pointing mouse.

2-D Finger-Pointing Mouse

We have implemented a two-dimensional finger-pointing mouse on a laptop computer (Figure 7). The input device is activated by touching a small transmitter electrode with the fourth (little) finger of the left hand. Energy is coupled into the person, and the EF emitted from the pointing finger is sensed at two receiving electrodes. A thin uniform copper strip running across the top of the screen senses Y position, and a tapered strip along the side of the screen senses X position. The taper renders the electrode more sensitive to the EF emitted by the pointing finger and less sensitive to the field emitted by the arm. The shaped electrode physically implements an analog spatially varying signal gain. A third small receiving electrode, placed below the spacebar, allows the thumb of the left hand to generate click signals.

The pointing finger does not need to be in contact with, or even close to the screen, thereby avoiding screen smudges and occlusion of the cursor by the pointing finger. Position sensing is easily disabled by lifting the forth finger off the transmitting electrode, the equivalent of lifting and putting down a mouse, facilitating relative position control.

Smart Table

To demonstrate the concept of "smart furniture," a co-linear dipole pair (i.e., receiver, transmitter, receiver) is placed underneath a wooden table to measure hand gestures. A computer screen displays an electronic newspaper whose pages are flipped forward and backward by sweeps of a hand across the table (X-axis). Placing the hand down on the table (Z-axis) advances to the next section, lifting the hand up displays the previous section. Gestures are detected by applying a threshold to the X and Z velocities. Position in the X-axis is approximated by differencing the two receiver signals; position in the Z-axis is approximated by the sum of the receiver signals.

An array of dipoles can turn a table into a multidimensional digitizing and gesture input device. Such an EF sensing matrix may substitute for or augment a video camera for video desk applications [18]. Perhaps visual ambiguities and occlusions could be arbitrated by EF sensing, indicating hand location to the video analysis system.

Person-Sensing Room

In an installation piece at the MIT Media Lab, a single transmitter electrode covers the entire floor of a room, coupling energy into a person walking on the floor. Four receiver electrodes, located on the walls, measure relative signal strength, indicating the location of the person. A computer program, controlling a multitude of synthesizers and sound sources, creates a complex sonic

terrain based on the location of the person, allowing navigation of a sonic environment.

Smart Chair

A chair is fitted with one transmitter in the seat and four receivers: two located in the headrest to measure head rotation, and one at each armrest to measure hand proximity. A person in the chair navigates multiple audio channels by head and hand placement [16]. The sensors are mounted underneath the chair fabric, so they are invisible to the user. Smart chairs may be used to control radio functions in a car, home audiovisual equipment, or simply to turn off a computer monitor when a user leaves a workstation.

In another application, a transmitter is installed in a chair to allow the magicians Penn & Teller to perform music by waving their arms near four receivers. Hand position controls various sound parameters produced by computer-controlled sound synthesizers.

Haptic Feedback in 3-D Space

A foam pad is placed on top of a dipole pair. Pressing on the foam produces a force feedback. Since force is proportional to position (Hooke's law), and finger position is measured by EF sensing, finger force is measured. A passive piece of foam on an EF sensor is a pressure sensor.

A plastic box is fitted with electrodes on three sides to measure hand position in 3-D. The box is filled with bird-seed (millet) to provide a viscous medium for haptic feedback. The seed allows users to rest their hand in space, reducing fatigue, and provides something to grab. Slight compression of the seed increases viscosity. Perhaps a computer-controlled piston, bearing on a movable wall of the box, could provide a simple way to simulate an environment with variable viscosity.

FUTURE APPLICATIONS

Researchers are currently exploring direct manipulation of instrumented real objects to facilitate 3-D orientation and manipulation [9, 17]. Electric field sensors may be incorporated in objects to measure object deformation, position, and orientation.

The Tailor project [20] allows disabled individuals to run computer applications by mapping the unique anatomical movement ability of each individual to control signals. Combining EF sensing with such mapping techniques could provide a person in a wheelchair with individually tailored, unobtrusive, invisible, low-power, and low-cost computer and machine interfaces.

Hermetically sealed EF sensors in a palm top could determine when the case is open, when the unit is being held, and could create a large control space around the small device. Foam EF buttons could provide force and tactile feedback, detect finger approach and finger pressure, and distinguish between slow and fast presses.

Multiple transmitters and receivers, multiplexed in time, frequency, or by coding sequence, could be placed under a carpet to determine the number and location of people in a room. When an electrode under a person is activated, that person becomes the EF source. Smart floors can be used for multi-participant VR simulations without the burden of wires or the complexities of video cameras.

Attempts have been made to instrument whiteboards using video cameras [11] and optoelectronics [2]. Both systems require rear imaging to record stylus movement. A conventional plastic whiteboard can be fitted with an array of EF sensing electrodes to measure the location of a metal-cased marker in the hand of a shunting or transmitting person.

Watches have a very small workspace and very little energy capacity. An EF sensor can be used to create a large workspace over a small watch face. Such watch controllers can be used to search through audio databases.

CONCLUSION

We have discussed some HCI systems and future applications of EF based sensing. The near-field nature of low-frequency electric fields allows the same detection scheme to be scaled from microns to meters. EF sensing provides high resolution proximity information. The difficulty is converting proximity to position. We have worked out an analytical method to correct for the non-uniform nature of dipole fields. Empirical methods may be used to compensate for complex field distortion caused by dielectrics or conductors in the field. Some of EF sensing's greatest qualitative appeals are the sense of magic, simplicity, and "naturalness" it brings to an HCI. The abilities of weakly electric fish to perform object detection, communicating, and jamming avoidance demonstrate what is possible with EF sensing. The authors know of no other sensing mechanism or system that can deliver non-contact sensing with millimeter resolution at kilohertz sample rates and millisecond lag times for a few dollars a channel. As computing power leaps off the desk and into a multitude of small battery-powered devices, the need for low-power unobtrusive interfaces grows. It is our belief that EF sensing can make a significant contribution to the sensing abilities of computing machines.

ACKNOWLEDGMENTS

The authors would like to thank Henry Chong for his programming assistance, the team of Teresa Marrin, Pete Rice, Edward Hammond, John Crouch, Ryan Christensen, and Alexander Sherstinsky for their work on the person-sensing room, and the Hewlett-Packard Corporation and the "News in the Future" consortium for their support.

REFERENCES

1. Bullock, T.H. Electroreception. Ann. Rev. Neuroscience, Vol. 5 (1982), pp. 121-170.

2. Elrod, S., et. al. Liveboard: A Large Interactive Display Supporting Group Meetings, Presentations and Remote Collaboration. CHI' 92Human Factors in Computing Systems (Monterey, May 3-7, 1992), ACM Press, pp. 599-607.

3. Federal Communications Commission, Part 15 Radio Frequency Devices. FCC, Washington, D.C.

4. Foster, R. Linear Capacitive Reactance Sensors for Industrial Applications. SAE Technical Paper 890974, 40th Annual Earthmoving Industry Conference, Peoria, Ill. (April 11-13, 1989).

5. Fraden, J. AIP Handbook of Modern Sensors, American Institute of Physics, New York, 1993, pp. 312-346.

6. Franklin, R. Fuller, F., Electronic Wall Stud Sensor. U.S. Patent No. 4,099,118, July 4, 1978.

7. Garner, L. For That Different Sound, Music a'la Theremin. Popular Electronics (November 1967), pp. 29-33,102-103.

8. Gershenfeld, N. Method and Apparatus for Electromagnetic Non-Contact Position Measurement with Respect to One or More Axes. U.S. Patent No. 5,247,261, Sept. 21, 1993.

9. Hinckley, K., et. al. Passive Real-World Interface Props for Visualization. CHI' 94Human Factors in Computing Systems (Boston, April 24-28, 1994), ACM Press, pp. 452-458.

10. Horowitz, P., Hill, W. The Art of Electronics, Cambridge University Press, New York, 1989, p. 889.

11. Ishii, H., Kobayashi, M. ClearBoard: A Seamless Medium for Shared Drawing and Conversation with Eye Contact. CHI'92 Human Factors in Computing Systems (Monterey, May 3-7, 1992), ACM Press, pp. 525-540.

12. Jackson, J. Classical Electrodynamics. John Wiley & Sons, New York, 1975, p. 138 and 392.

13. Lee, S., Buxton, W., Smith, K. A Multi-touch Three Dimensional Touch-Sensitive Tablet. CHI'85 Human Factors in Computing Systems (1985) ACM Press, pp. 21-24.

14. Mathews, M. Three Dimensional Baton and Gesture Sensor. U.S. Patent No. 4,980,519, Dec. 25, 1990.

15. Meyer, K., Applewhite, H., A Survey of Position Trackers. Presence, Vol. 1, No. 2 (Spring 1992), MIT, pp. 173-200.

16. Mullins, A. AudioStreamers: Browsing Concurrent Audio Streams. Master's Thesis, MIT Media Lab, June 1995 (forthcoming).

17. Murakami, T. Nakajima, N., Direct and Intuitive Input Device for 3-D Shape Deformation. CHI'94 Human Factors in Computing Systems (Boston, April 24-28, 1994), ACM Press, pp. 465-470.

18. Newman, W, Wellner, P. A Desk Supporting Computer-Based Interaction with Paper Documents. CHI' 92 Human Factors in Computing Systems (Monterey, May 3-7, 1992), ACM Press, pp. 587-598.

19. Paradiso, J. A Simple Technique for Measuring Axial Displacement in Stretched-Wire Alignment Systems. (May 1994), Draper Technical Report GEM-TN-94-607, Cambridge, Massachusetts.

20. Pausch, P., et. al. One-Dimensional Motion Tailoring for the Disabled: A User Study. CHI' 92Human Factors in Computing Systems (Monterey, May 3-7, 1992), ACM Press, pp. 405-411.

21. Webster, J.G. Electrical Impedance Tomography, Adam Hilger, Bristol, 1990, pp. 1.

22 Vranish, J. McConnell, R., Driven Shielding Capacitive Proximity Sensor. U.S. Patent No. 5,166,679, Nov. 24, 1992.

Application Serial No. 11/380,109
Filed on April 25, 2006

DOCKET NO: P4046US1
(119-0089US)

APPLICATION

FOR

UNITED STATES LETTERS PATENT

TITLE: **Keystroke Tactility Arrangement On A Smooth Touch Surface**

INVENTOR: **WAYNE CARL WESTERMAN**
San Francisco, California

Prepared by: WONG, CABELLO, LUTSCH, RUTHERFORD & BRUCCULERI, L.L.P.
Houston, Texas

KEYSTROKE TACTILITY ARRANGEMENT ON A SMOOTH TOUCH SURFACE

CROSS-REFERENCE TO RELATED APPLICATIONS

[0001] This application is related to the following patents and patent applications, which are all herein incorporated by reference: (1) U.S. Patent No.: 6,323,846, titled "Method and Apparatus for Integrating Manual Input," issued on July 1, 2002; (2) U.S. Patent No.: 6,677,932, titled "System and Method for Recognizing Touch Typing Under Limited Tactile Feedback Conditions," issued on January 13, 2004; and (3) U.S. Patent No.: 6,570,557, titled "Multi-Touch System and Method for Emulating Modifier Keys Via Fingertip Chords," issued on May 27, 2003.

BACKGROUND

[0002] Integration of typing, pointing, and gesture capabilities into touch surfaces offers many advantages, such as eliminating need for mouse as a separate pointing device, eliminating wasteful reaches between keyboard and pointing device, and general workflow streamlining. However, pointing and typing have opposite tactile feedback needs. Specifically, pointing and gesturing inputs are best accomplished using a smooth, nearly frictionless touch surface. Conversely, typists are accustomed to relying on sharp key edges for tactile feedback.

[0003] User acceptance of the TouchStream™ integrated typing, pointing and gesture input devices manufactured by FingerWorks demonstrated that learning to type on a smooth, un-textured surface is possible, but takes substantial practice. In many ways, typing on such a surface is almost like learning to type all over again. It is believed that mainstream acceptance of typing on touch surfaces will require shortening of the typing re-acclimation period, which, in turn, requires improved keystroke tactility.

[0004] Traditionally, keystroke tactility on a surface or "membrane" keyboard has been provided by indicating key edges using hydroformed or stamped raised ridges into the surface plastic. However, this technique has several disadvantages for touch

surfaces also intended for pointing and gesture. For example, the key-edge ridges impede lateral pointing motions, giving the surface a rough washboard feel. The ridges also disrupt position interpolation from capacitive sensor arrays as the fingertip flesh lifts over the ridge.

[0005] In a more successful attempt to provide surface keyboard users with suitable tactile feedback, keyboards incorporating home row dimples as disclosed in U.S. Patent 6,323,846, referenced above, were produced. These dimples helped users find the home row keys when hands were resting on the surface, while minimizing disruption of a user's motion in pointing or gesturing on the surface. However, these dimples were ineffective feedback for helping users feel for keys away from home row, or detect when they were not striking the centers of these peripheral keys.

[0006] Another somewhat successful prior method for aligning hands on both surface and traditional mechanical keyboards has been to place a single raised Braille-like dot on an "alignment" key or on the "home row" of keys. For example, many mechanical keyboards features such raised dots on the "F" and "J" keys, which are the index finger home positions for a touch typist using QWERTY keyboard. As with the dimples disclosed in the '846 patent, this arrangement is useful to help align a user's hands to home row, but does not help to correct alignment errors while reaching for peripheral keys. Thus, a significant problem arises in attempting to provide feedback of key positions away from the home row.

[0007] Placing alignment dots, such as the single Braille-like dot, at the center of every key would provide feedback for key positions away from the home row. However, such an arrangement would eliminate the distinctiveness of the home row keys, and create more ambiguous feedback for the user. Therefore, what is needed in the art is a way to provide tactility to all or at least a substantial number of keys without creating such a bumpy surface that pointing and gestures are uncomfortable or unsteady.

[0008] This could be accomplished by adapting known prior art Braille displays. In this approach, tiny, individually actuated pins spread across the keyboard could

provide dynamic tactility, but at great mechanical cost and complexity. Thus, what is needed to reduce cost and complexity is a way to provide tactility for each key without placing individual electromagnetic actuators under each key.

[0009] An additional issue arises in that multi-touch capacitive sensor arrays, which are often used to form the multi-touch surfaces, are typically built with row and column electrodes spanning the surface, or with row and column drive/sense line accessing electronic buffers at each electrode cell. Thus whatever tactility mechanism is provided, the arrangement must be routable around the row/column electrodes or drive lines of multi-touch sensors without requiring additional circuit board vias or layers.

[0010] Disclosed herein are a variety of techniques for providing tactile feedback in a surface or other keyboard that address one or more of these deficiencies of the prior art.

SUMMARY

[0011] Disclosed herein are four arrangements for providing tactility on a touch surface keyboard. One approach is to provide tactile feedback mechanisms, such as dots, bars, or other shapes on all or at least many keys. Different keys or groups of keys may have different feedback mechanisms, *e.g.*, a first feedback mechanism may be assigned to "home row" keys, with a second feedback mechanism assigned to keys adjacent the home row, with a third assigned to peripheral keys, which are neither home row keys nor adjacent the home row. Alternatively, an articulating frame may be provided that extends when the surface is being used in a typing mode and retracts when the surface is used in some other mode, *e.g.*, a pointing mode. The articulating frame may provide key edge ridges that define the boundaries of the key regions or may be used to provide tactile feedback mechanisms within the key regions. The articulating frame may also be configured to cause concave depressions similar to mechanical key caps in the surface. In another embodiment, a rigid, non-articulating frame may be provided beneath the surface. A user will then feel higher resistance

when pressing away from the key centers, but will feel a softer resistance, which may be enhanced by filling the gaps with a foam or gel material or air.

[0012] Using these arrangements, as well as individual elements of each or combinations thereof, it is possible to provide strong tactile feedback of each key location without impeding pointing, gestures, or related lateral sliding motions on the same touch surface.

BRIEF DESCRIPTION OF THE DRAWINGS

[0013] The invention may best be understood by reference to the following description taken in conjunction with the accompanying drawings in which:

[0014] Figure 1 is a top view of a surface keyboard employing a tactile feedback mechanism.

[0015] Figure 2 is a cross-section view of the surface keyboard depicted in Fig. 1.

[0016] Figure 3 is a top view of a surface keyboard employing a variation of the tactile feedback mechanism depicted in Figs. 1 and 2.

[0017] Figure 4 is a cross-section view of the surface keyboard depicted in Fig. 3.

[0018] Figure 5 is a cross-section view of a surface keyboard employing an alternative tactile feedback arrangement including an articulating frame (shown in an extended position).

[0019] Figure 6 is a cross-section view of the surface keyboard illustrated in Fig. 5 with the articulating frame shown in a retracted position.

[0020] Figure 7 is a plan view of the surface keyboard illustrated in Figs. 5 and 6.

[0021] Figures 8A and 8B illustrate a cross-section view of a surface keyboard tactile feedback arrangement for simulating concave key cap centers.

[0022] Figure 9 illustrates a cross-section view of a surface keyboard employing a deformable material beneath the keys to provide tactile feedback.

DETAILED DESCRIPTION

Braille-Like Dot Pairs Or Bars At Key Centers

[0023] With reference now to Figs. 1 and 2, one technique for providing tactile feedback in a surface keyboard is depicted. Figure 1 is a vertical view of a surface keyboard 100. Figure 2 is a cross-section view of surface keyboard 100. Surface keyboard 100 includes numerous key regions 101. As used herein, the term "key" may also refer to the key regions 101, although in a surface keyboard there is actually no mechanical key. Rather, sensing circuitry 111 disposed beneath the surface cover 112 detects an object, such as a user's finger, in contact or close proximity with the key regions 101 and outputs the corresponding letter, number, or symbol to a host computer or other device (not shown). The key layout shown in Fig. 1 is a slightly modified QWERTY layout, which has been ergonomically designed to provide a more comfortable typing position.

[0024] Key regions 101 are arranged in a plurality of rows. As known to touch typists, the row of keys containing the letters "ASDF" on the left-hand side and "JKL;" on the right-hand side are known as the home row 102. The home row is so called because a touch typist will keep the four fingers of each hand over these characters when a finger is not reaching for a key in another row. Adjacent rows 103 are the rows immediately adjacent, for example, the rows containing "QWER" and "ZXCV." The remaining rows are known as peripheral rows 104, for example, the row of number keys.

[0025] One mechanism to provide more robust tactile feedback for a user of a surface keyboard is to stamp two horizontally aligned dots 105 at the center of each home row key 106. Similarly, two vertically aligned dots 107 may be stamped on each adjacent key 108. Finally, a single dot 109 may be stamped on peripheral keys 110. Because the home row keys feel different than all other keys, home row 102 may be easily found without looking when sliding hands over the surface. The two vertical dots

107 on adjacent keys 108 in turn help distinguish their feel from peripheral number and punctuation keys having only one raised dot 110.

[0026] It will be appreciated that the particular arrangement of dots could vary from that described. For example, a single dot could be used to mark home row keys 102, with two horizontal dots used for adjacent keys 103 and two vertical dots used for peripheral keys 104. All that is required is that one unique tactile feedback mechanism, such as raised dots, be used for home row keys, while another is used for adjacent and/or peripheral keys. It is not required that the adjacent keys and peripheral keys employ different tactile feedback mechanisms, although it may be preferable to do so.

[0027] Moreover, the tactile feedback mechanism need not be limited to raised dots. In a variation of this technique, shown in plan-view in Fig. 3 and in cross-section in Fig. 4, the a raised dot pair is replaced with a raised "hyphen," *i.e.*, a short bar 113. The short bars 113 may be, for example, arranged horizontally (113a) at the centers of home row keys 106 and vertically (113b) on keys adjacent to home row 102. Peripheral keys 110 may include a single raised dot 109. Other shapes, such as squares, circles, triangles, etc. could also be used so long as the arrangements used for home row keys 102 are distinct from those used for the adjacent keys 103 and/or peripheral keys 104. These embodiments may be less desirable than a raised dot pair in terms of efficient tactility and minimizing sensor distortion. However, these raised bars or other shapes may be more aesthetically pleasing than raised dot pairs.

[0028] It should also be noted that, although the tactile feedback arrangement described above has particular applicability to surface keyboards, it could also be used in conjunction with traditional mechanical/electromechanical keyboards. Additionally, although described in terms of the traditional QWERTY keyboard, the techniques may also be applied to other keyboard layouts, such as Dvorak keyboard, foreign language keyboards, court reporting machine keyboards, and other keyboard-like input devices.

Articulating Frame Protrudes At Key Edges During Typing

[0029] An alternative technique for providing tactile feedback in a surface keyboard will now be described with respect to Figs. 5, 6, and 7. Figures 5 and 6 depict a cross-section view of the keyboard, while Fig. 7 depicts a plan view. As illustrated in Figs. 5 and 6, the surface keyboard 200 comprises a plurality of layers including an enclosure base 201, the electrode circuit board 202, and the surface cover 203. Details of the construction of these devices are described in the various incorporated references and are not repeated here.

[0030] Additionally, the keyboard 200 includes an articulating frame 204, which is disposed beneath the circuit board 202. The articulating frame 204 may be raised and lowered by actuators 205, which preferably take the form of electromagnetic actuators. Raising and lowering the articulating frame extends and withdraws key edge ridges 206, which are dots or bars that poke through the keyboard surface when extended. Electromagnetic actuators 205 would raise the frame when operating in a typing mode such that the tops of the key edge ridges 206 are about 1mm above the surface cover 203. The electromagnetic actuators 205 would lower the frame when operating in a pointing/gesture mode such that the tops of the key edge ridges 206 are flush with surface cover 203, thereby providing a substantially smooth surface for pointing and gesturing. Although electromagnetic actuators 205 are depicted as being disposed beneath the frame and above the enclosure bottom, they may be disposed in any arrangement that allows them to suitably displace the frame 204 and key edge ridges 206.

[0031] Preferably, each key edge comprises one to four distinct bars or Braille-like dots. When constructed in conjunction with a capacitive multi-touch surface, the key edge ridges should separated to accommodate the routing of the drive electrodes, which may take the form of rows, columns, or other configurations. As an alternative to key edge ridges 206, the frame could cause Braille-like dots or similar markers, as discussed above with respect to Figs. 1–4 to protrude through the key centers, although this arrangement would potentially interfere with touch detection and

measurement because it would require mechanical devices in proximity to the key center, which is a preferred sensor location. In yet another alternative arrangement, articulating frame 204 could be disposed above the electrode circuit board 202, although the added separation between the surface cover 203 and the circuit board 202 could complicate the touch measurement and detection.

[0032] The electromagnetic actuators may be located at the corners and/or center of the frame or distributed variously throughout the frame. Selection of a particular position will necessitate the determination of a variety of design parameters, such as frame material strength, power routing, cost, etc., all of which would be within the abilities of one skilled in the art having the benefit of this disclosure. The actuators 205 may be activated manually, for example, by touching the surface in a particular region, pressing a dedicated button, activating a switch, etc. Alternatively, the actuators raise and lower the frame according to mode commands from gesture and typing recognition software, such as that described in the '846 patent incorporated by reference above.

[0033] Specifically, the recognition software commands lowering of the frame when lateral sliding gestures or mouse clicking activity chords are detected on the surface. Alternatively, when homing chords (*i.e.*, placing the fingers on the home row) or asynchronous touches (typing activity) is detected on the surface, the recognition software commands raising of the frame. Various combinations or subsets of these recognition techniques could also be used. For example, the device may activate a typing mode when homing chords or asynchronous touches are detected and deactivate the typing mode if neither is detected for a some time interval. In this configuration the device effectively defaults to a pointing mode and switches to a typing mode when necessary. Conversely, the device could activate a pointing mode when lateral sliding gestures or mouse clicking activity is detected and switch to a typing mode when these activities are not detected for some time interval. In any case, the frame will change modes automatically from lowered and flush (pointing mode) to poking through the surface (typing mode) as often as the operator switches between pointing and typing.

Of course, operators who did not like the automated behavior could manually toggle the frame state with a pre-assigned gesture.

[0034] When extended, the key edge bars 206 provide similar tactile feel to a conventional mechanical key edge when the finger straddles two keys. However, this arrangement does not effectively simulate the concave depression common in mechanical keycaps, which helps a typists fingers sink towards the key center. Obviously, the key edge bars 206 will only be felt if fingers touch way off key center. Additionally, the holes in surface cover 203 through which the key edge bars 206 extend may collect dirt and grime. However, an extension of this arrangement may be used to address these concerns.

Articulating Frame Deforms Surface Cover at Key Edges During Typing

[0035] Illustrated in Figs. 8A and 8B is a variation of the articulating frame arrangement discussed above with respect to Figs. 5, 6, and 7. Figure 8A shows the frame in the raised (typing) position, while Figure 8B shows the frame in the lowered (pointing, gesturing, etc.) position. In this embodiment, the bars of articulating frame 304 protrude through the circuit board 302, but not through the surface cover 303. When actuators 305, disposed between enclosure base 301 and the articulating frame 304 raise frame 304, the bars 306 lift the surface cover 303, rather than poking through. By tacking the surface cover 303 to the circuit board 302 at the key centers, a concave keycap depression effect 307 will be created when the frame raises. This allows a users fingers to be guided toward the center of each key, much like a conventional keyboard. Additionally, because there are no holes in the surface cover 303, there is likely to be less accumulation of dirt and grime on the surface. Obviously, such an arrangement requires a more supple cover material than the rigid Lexan (polycarbonate) sheets often used as touchpad surfaces, but a variety of such materials are well known to those skilled in the art.

Rigid Frame Under Key Edges with Compressible Key Centers

[0036] Yet another embodiment may extends the covered key edge bars and key center depressions while dispensing with the mechanical complexity of frame articulation. Such an embodiment is illustrated in Fig. 9. The surface keyboard 400 comprises the familiar layers of an enclosure base (not shown), sensing circuit board 402 (with electrodes 402a), and surface cover 403. The surface cover sits atop a frame including a fixed network of hard key-edge ridges 404, which are preferably raised about 0.5–1mm above the sensing circuit board 402. The gaps between the key edge ridges 404 are filled with a compliant gel or foam material 405 (or possibly even air) filling the key centers up to flush with the ridges.

[0037] This arrangement allows the surface cover 303 to drape substantially perfectly flat, and remain flat when under light pressure, *e.g.*, that from a pointing or dragging operation. However, when a user presses a key center, the cover would give under their finger somewhat as the foam/gel/air material 405 is compressed, while a user pressing over a key edge would feel the hard ridge underneath. While this arrangement is electrically and mechanically simple (with no active mechanical parts), the surface cover and key filler materials must be chosen carefully to provide noticeable compression at key center yet be durable to wear. Additionally, the sandwich of surface cover and foam could become too thick for the capacitive sensors to properly detect through. To overcome these deficiencies, the surface cover 303 itself could contain flex circuitry (well known to those skilled in the art) imprinted with a suitable electrode pattern, which would dispense with the necessity of the electrode layer 402.

[0038] Many variations and/or combinations of the embodiments discussed herein will be apparent to those skilled in the art. For example, as noted above, the articulating frame may be combined with the Braille-like dots to form articulating Braille-like dots. Alternatively, the fixed Braille-like dots may be combined with the articulating ridges described with reference to Fig. 8 or with the compressible material of Fig. 9. It should also be noted that there are many alternative ways of implementing the

methods and apparatuses of the present invention. It is therefore intended that the following appended claims be interpreted as including all such alterations, permutations, combinations and equivalents as fall within the true spirit and scope of the invention.

CLAIMS

What is claimed is:

1. A keyboard having a tactile feedback arrangement, the tactile feedback arrangement comprising:

   a first tactile feedback mechanism for each home row key; and

   an additional tactile feedback mechanism distinct from the first tactile feedback mechanism for at least one key adjacent a home row key or at least one peripheral key.

2. The keyboard of claim 1 wherein the additional tactile feedback mechanism comprises:

   a second tactile feedback mechanism for at least one key adjacent the home row keys; and

   a third tactile feedback mechanism for at least one peripheral key;

   wherein the second and third tactile feedback mechanisms are distinct from each other.

3. The keyboard of claim 2 wherein:

   the second feedback mechanism is provided for each key adjacent a home row key; and

   the third feedback mechanism is provided for each peripheral key.

4. The keyboard of claim 1, 2, or 3 wherein the tactile feedback mechanisms are selected from the group consisting of: a single raised dot, two raised dots arranged horizontally, two raised dots arranged horizontally, a raised bar oriented horizontally, and a raised bar oriented vertically.

5. The keyboard of claim 4 wherein the keyboard is a multi-touch surface.

6. The keyboard of claim 5 wherein the feedback mechanism is stamped into a cover of the multi-touch surface.

7. A touch sensitive surface configurable to operate as a keyboard, the touch sensitive surface comprising:

a surface cover;

a touch sensitive electrode circuit board disposed beneath the surface cover having a plurality of holes disposed therein;

an articulating frame disposed beneath the touch sensitive electrode circuit board having integral therewith a plurality of key edge ridges aligned with the holes in the touch sensitive electrode; and

at least one actuator disposed between the articulating frame and an enclosure of the touch sensitive surface and configured to displace the articulating frame so as to extend the key edge ridges through the holes in the touch sensitive electrode circuit board.

8. The touch sensitive surface of claim 7 wherein the surface cover includes a plurality of holes aligned with the holes in the circuit board and wherein the actuator is configured to displace the articulating frame so as to extend the key edge ridges through the holes in the surface cover.

9. The touch sensitive surface of claim 7 wherein the surface cover is attached to the touch sensitive electrode circuit board at a center of a key region such that extending the key edge ridges through the holes in the touch sensitive electrode circuit board forms a concave depression within the key region.

10. A touch sensitive surface according to any of claims 7, 8, or 9 wherein the key edge ridges are extended when the device operates in a typing mode and retracted when the devices operates in a pointing mode.

11. The touch sensitive surface of claim 10 wherein switching between typing mode and pointing mode is accomplished manually.

12. The touch sensitive surface of claim 11 wherein manual switching is accomplished by at least one of: actuating a switch, pressing a button, touching the surface in a pre-defined region, and performing a pre-determined gesture.

13. The touch sensitive surface of claim 10 wherein switching between typing mode and pointing mode is accomplished automatically.

14. The touch sensitive surface of claim 13 wherein at least one of the following:
the typing mode is activated when asynchronous touches are detected;
the typing mode is deactivated when asynchronous touches are no longer detected;
the typing mode is activated when homing chords are detected;
the typing mode is deactivated when homing chords are no longer detected;
the pointing mode is activated when lateral sliding gestures are detected;
the pointing mode is deactivated when lateral sliding gestures are detected;
the pointing mode is activated when mouse clicking activity chords are detected; and
the pointing mode is deactivated when mouse clicking activity chords are detected.

15. The touch sensitive surface of claim 10 wherein the key edge ridges comprise a plurality of distinct bars or dots.

16. The touch sensitive surface of claim 7 or 8 wherein the key edge ridges comprise tactile feedback mechanisms located at a center of one or more key regions.

17. The touch sensitive surface of claim 16 wherein the tactile feedback mechanisms are selected from the group consisting of: a single raised dot, two raised dots arranged horizontally, two raised dots arranged horizontally, a raised bar oriented horizontally, and a raised bar oriented vertically.

18. The touch sensitive surface of claim 16 wherein the tactile feedback mechanisms comprise:

a first tactile feedback mechanism for each home row key; and

an additional tactile feedback mechanism distinct from the first tactile feedback mechanism for at least one key adjacent a home row key or at least one peripheral key.

19. The touch sensitive surface of claim 18 wherein the additional tactile feedback mechanism comprises:

a second tactile feedback mechanism for at least one key adjacent the home row keys; and

a third tactile feedback mechanism for at least one peripheral key;

wherein the second and third tactile feedback mechanisms are distinct from each other.

20. The keyboard of claim 19 wherein:

the second feedback mechanism is provided for each key adjacent a home row key; and

the third feedback mechanism is provided for each peripheral key.

21. A touch sensitive surface configurable to operate as a keyboard, the touch sensitive surface comprising:

a surface cover;

a touch sensitive electrode circuit board disposed beneath the surface cover;

a frame disposed between the touch sensitive electrode circuit board and the surface cover, the frame comprising a fixed network of hard key edge ridges; and

a compliant material filling gaps between the key edge ridges.

22. The touch sensitive surface of claim 21 wherein the compliant material is selected from the group consisting of: a gel, a foam, and air.

23. The touch sensitive surface of claim 21 or 22 comprising one or more tactile feedback mechanisms stamped into the surface cover.

24. The touch sensitive surface of claim 23 wherein the one or more tactile feedback mechanisms are selected from the group consisting of: a single raised dot, two raised dots arranged horizontally, two raised dots arranged horizontally, a raised bar oriented horizontally, and a raised bar oriented vertically.

25. The touch sensitive surface of claim 24 wherein the one or more feedback mechanisms comprise:

a first tactile feedback mechanism for each home row key; and

an additional tactile feedback mechanism distinct from the first tactile feedback mechanism for at least one key adjacent a home row key or at least one peripheral key.

26. The touch sensitive surface of claim 25 wherein the additional tactile feedback mechanism comprises:

a second tactile feedback mechanism for at least one key adjacent the home row keys; and

a third tactile feedback mechanism for at least one peripheral key;

wherein the second and third tactile feedback mechanisms are distinct from each other.

27. The keyboard of claim 26 wherein:

the second feedback mechanism is provided for each key adjacent a home row key; and

the third feedback mechanism is provided for each peripheral key.

KEYSTROKE TACTILITY ARRANGEMENT ON A SMOOTH TOUCH SURFACE

Abstract

Disclosed are four arrangements for providing tactility on a touch surface keyboard. One approach is to provide tactile feedback mechanisms, such as dots, bars, or other shapes on all or many keys. In another embodiment, an articulating frame may be provided that extends when the surface is being used in a typing mode and retracts when the surface is used in some other mode, *e.g.*, a pointing mode. The articulating frame may provide key edge ridges that define the boundaries of the key regions or may provide tactile feedback mechanisms within the key regions. The articulating frame may also be configured to cause concave depressions similar to mechanical key caps in the surface. In another embodiment, a rigid, non-articulating frame may be provided beneath the surface. A user will then feel higher resistance when pressing away from the key centers, but will feel a softer resistance at the key center.

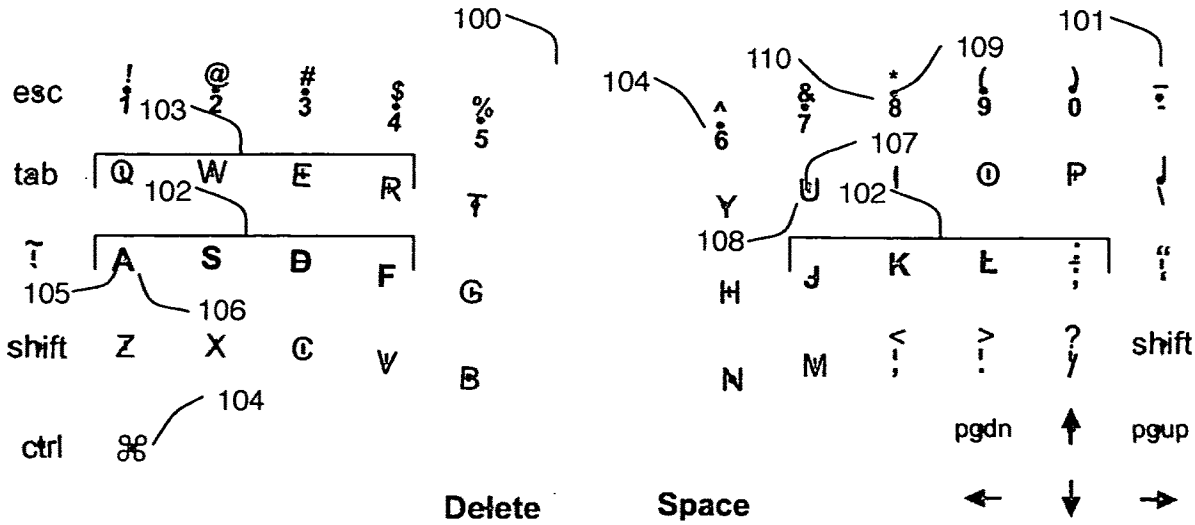

Fig. 1

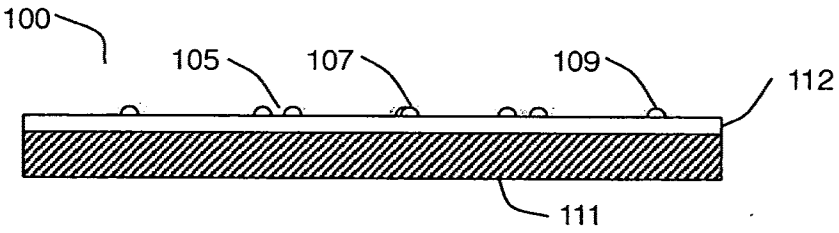

Fig. 2

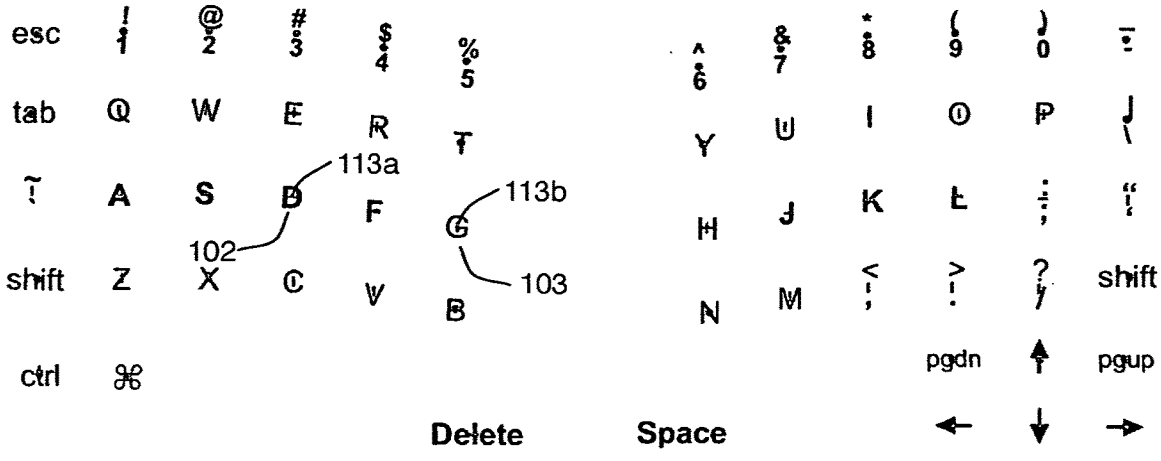

Fig. 3

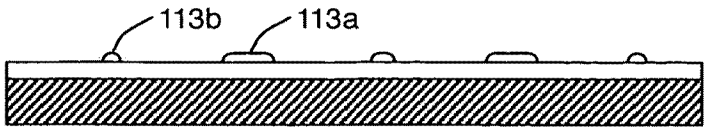

Fig. 4

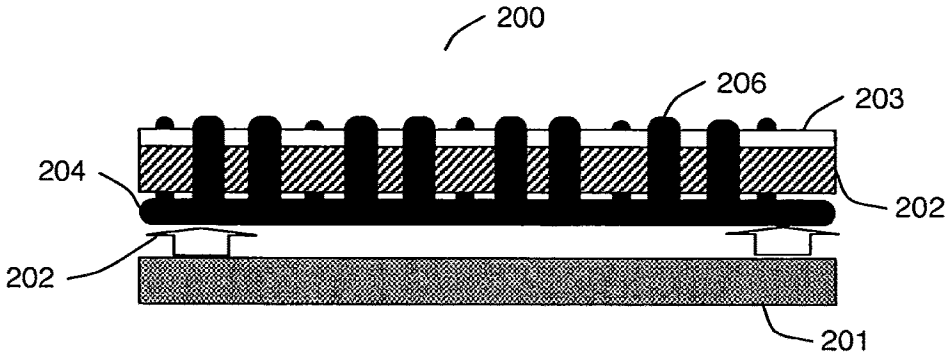

Fig. 5

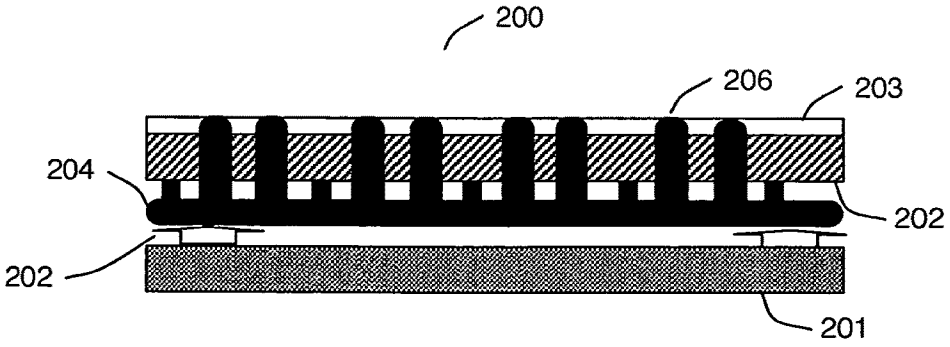

Fig. 6

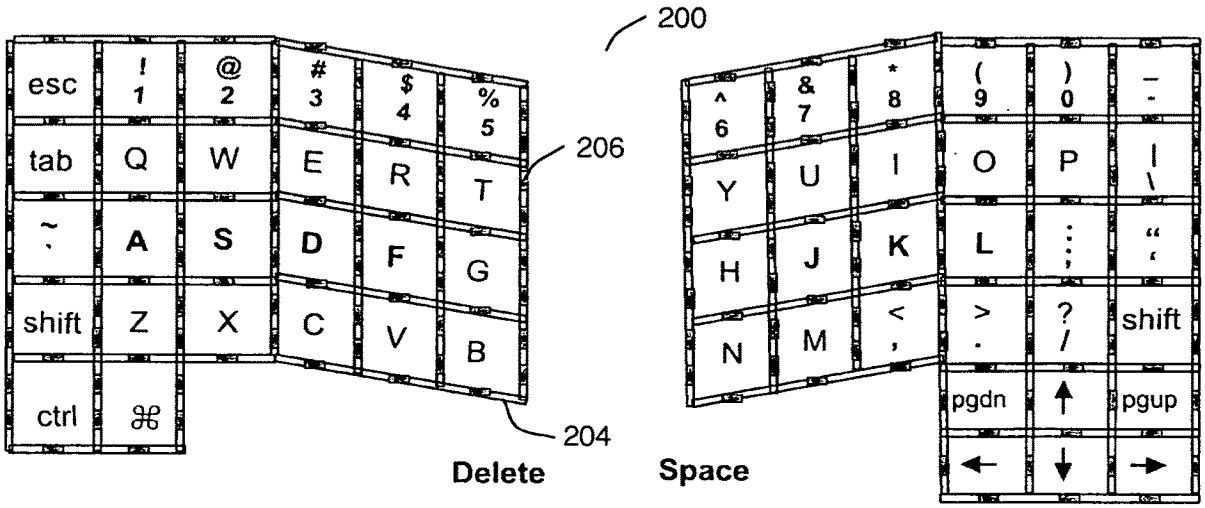

Fig. 7

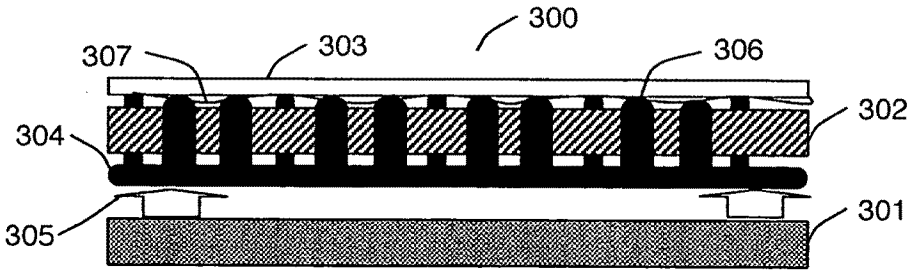

Fig. 8A

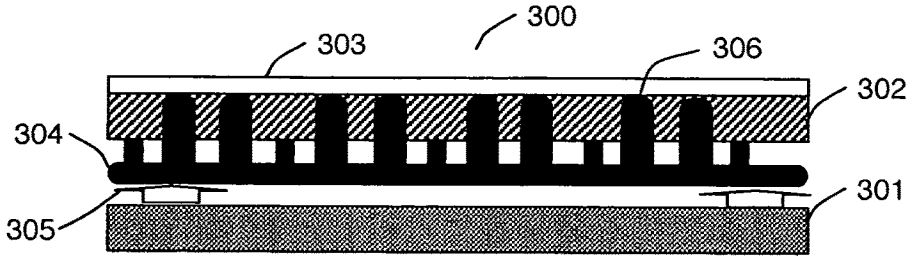

Fig. 8B

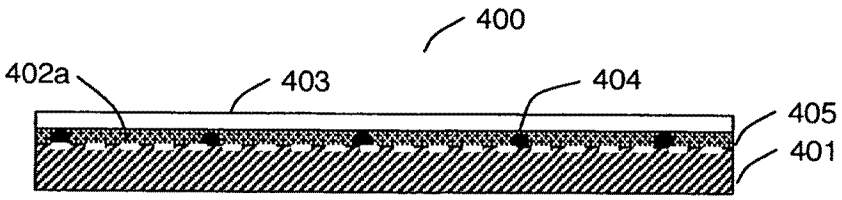

Fig. 9

Office de la Propriété Intellectuelle du Canada
Un organisme d'Industrie Canada

Canadian Intellectual Property Office
An agency of Industry Canada

CA 2318815 C 2004/08/10

(11)(21) 2 318 815

(12) BREVET CANADIEN
CANADIAN PATENT

(13) C

(86) Date de dépôt PCT/PCT Filing Date: 1999/01/25
(87) Date publication PCT/PCT Publication Date: 1999/07/29
(45) Date de délivrance/Issue Date: 2004/08/10
(85) Entrée phase nationale/National Entry: 2000/07/24
(86) N° demande PCT/PCT Application No.: US 1999/001454
(87) N° publication PCT/PCT Publication No.: 1999/038149
(30) Priorités/Priorities: 1998/01/26 (60/072,509) US; 1999/01/25 (09/236,513) US

(51) Cl.Int.^{6}/Int.Cl.^{6} G09G 5/00
(72) Inventeurs/Inventors:
WESTERMAN, WAYNE, US;
ELIAS, JOHN G., US

(73) Propriétaires/Owners:
WESTERMAN, WAYNE, US;
ELIAS, JOHN G., US

(74) Agent: BORDEN LADNER GERVAIS LLP

(54) Titre : PROCEDE ET DISPOSITIF D'INTEGRATION D'ENTREE MANUELLE
(54) Title: METHOD AND APPARATUS FOR INTEGRATING MANUAL INPUT

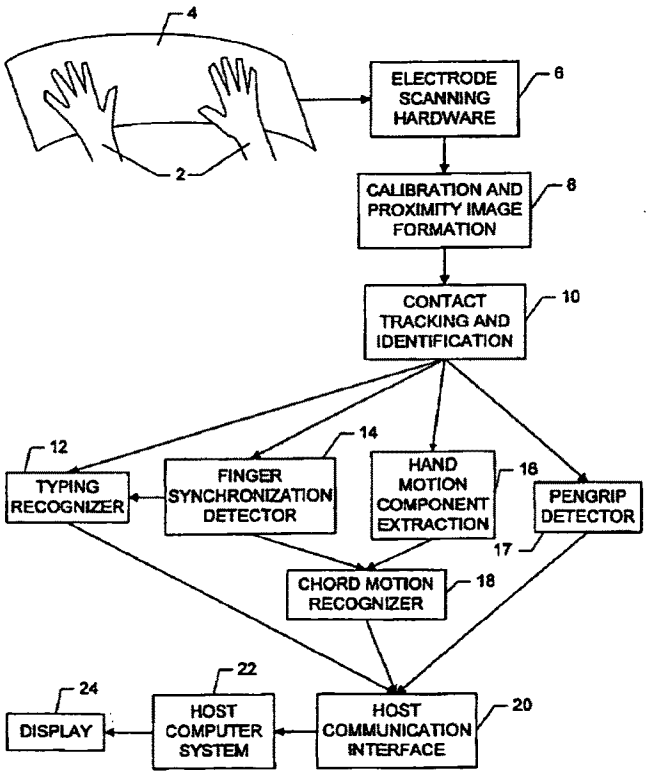

(57) Abrégé/Abstract:
Apparatus and methods are disclosed for simultaneously tracking multiple finger (202-204) and palm (206, 207) contacts as hands approach, touch, and slide across a proximity-sensing, compliant, and flexible multi-touch surface (2). The surface consists of compressible cushion (32), dielectric electrode (33), and circuitry layers. A simple proximity transduction circuit is

CA 2318815 C 2004/08/10
(11)(21) 2 318 815
(13) C

(57) Abrégé(suite)/Abstract(continued):
placed under each electrode to maximize the signal-to-noise ratio and to reduce wiring complexity. Scanning and signal off-set removal on electrode array produces low-noise proximity images. Segmentation processing of each proximity image constructs a group of electrodes corresponding to each distinguishable contacts and extracts shape, position and surface proximity features for each group. Groups in successive images which correspond to the same hand contact are linked by a persistent path tracker (245) which also detects individual contact touchdown and liftoff. Classification of intuitive hand configurations and motions enables unprecedented integration of typing, resting, pointing, scrolling, 3D manipulation, and handwriting into a versatile, ergonomic computer input device.

US Application Serial No. 10/774,053
Filed on February 5, 2004

HYBRID GROUND GRID FOR PRINTED CIRCUIT BOARD

By Inventors:

Robert J. Steinfeld
Cheung-Wei Lam

TECHNICAL FIELD

[0001] The invention described herein relates generally to printed wiring board layout. In particular, the invention relates to a printed circuit board construction having a hybrid grid network of ground traces formed on two or more layers of the printed circuit board to provide electrical paths capable of reducing Electromagnetic Emissions and improving the Electromagnetic Immunity performance as well as being capable of accommodating a wide range of component arrangements and signal trace configurations.

BACKGROUND

[0002] In conventional circuit mounting boards (e.g., printed circuit boards (PCB's)) a ground plane is formed on one or more layers of the board. Such ground planes can be formed on the top or bottom surfaces of boards (especially using basic two layer boards). Also, such ground planes can be formed on interior layers of multi-layer (three or more layers) boards. Such ground planes are satisfactory for certain purposes, but they impose certain significant design limitations. For example, they prohibit the formation of signal traces on the layer containing the ground plane. On a two-layer board this can be a particularly cumbersome design limitation because it effectively prevents circuit structures and electronic components from being formed on or attached to the ground plane layer. This cuts the available board space for such circuitry and components in half.

:: Home

TECHNOLOGIES

Capacitive Position Sensing
Capacitive Force Sensing
Transparent Capacitive Position Sensing
Inductive Position Sensing
Pattern Recognition
Mixed Signal VLSI
Proprietary Microcontroller
Briefs & Whitepapers

Capacitive Position Sensing

Synaptics is a world leader in capacitive touch sensing technology. This technology is at the heart of our industry-standard TouchPad products. Since the introduction of the TouchPad, we have expanded our technology in a variety of directions including pen sensors, force sensors, and flexible touch sensors.

How the TouchPad Works

Synaptics TouchPad devices work by sensing an electrical property called capacitance. Whenever two electrically conductive objects come near to each other without touching, their electric fields interact to form capacitance. The surface of a TouchPad sensor is an array of conductive metal electrodes, covered by a protective insulating layer. The human finger is also an electrical conductor, and when you place your finger on a TouchPad, a tiny capacitance forms between your finger and the metal electrodes in the TouchPad. The insulating layer protects the TouchPad sensor from wear by preventing your finger from actually touching the sensor, and is textured to help your finger move smoothly across the surface.

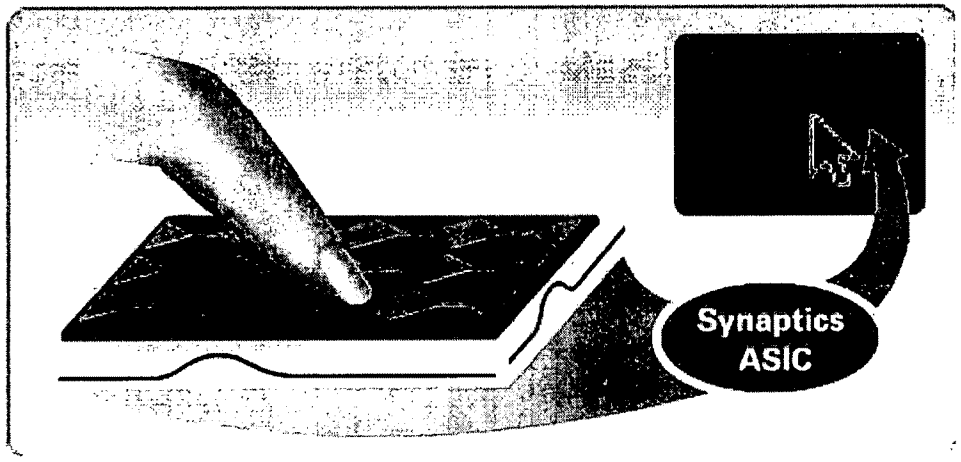

The TouchPad sensor's sensitive analog electronics measure the amount of capacitance in each of the electrodes. By sensing when the capacitance increases, the TouchPad can tell when your finger is touching. By measuring which electrodes have the most capacitance, the TouchPad can also locate your finger to an accuracy of better than 1/1000th of an inch. The capacitive sensing ASIC chip incorporates a

proprietary microprocessor that computes the finger's pos. . and speed and reports them to the host computer in the form of cursor motion.

On a PC, the TouchPad can work with any mouse driver, but it works best with the Synaptics TouchPad driver. When used with the Synaptics driver, the TouchPad reports not just the mouse-like motion of the finger, but also the absolute position of the finger on the TouchPad surface as well as the amount of finger pressure. The driver uses this extra information to enhance the user interface in a variety of ways. For example, if the finger moves up and down along the right-hand edge of the pad, the driver activates the patented Virtual Scrolling feature.

In addition, a general purpose TouchPad Application Programming Interface (API) is available in the Customer Support-Developer's Support section of the web site, which allows adaptation of our TouchPad into other products. The underlying capacitive technology in the TouchPad can be developed for a wide variety of devices, such as cell phones, MP3 players, PDAs, touchscreens, and remote controls. Synaptics capacitive sensing technology has been used to provide 2D cursor control, 1D scrolling functionality, and replace electrical switches in many types of electronic devices.

Synaptics' capacitive sensing technology has numerous advantages over competing technologies like membrane switches and resistive sensors. Its solid-state construction makes it extraordinarily rugged. And because our capacitive sensor is so versatile, it can be made extremely thin, lightweight, flexible, or even transparent. The proprietary microprocessor makes it possible to build custom capacitive solution for special applications.

TouchScreens.com

Capacitive Touchscreens

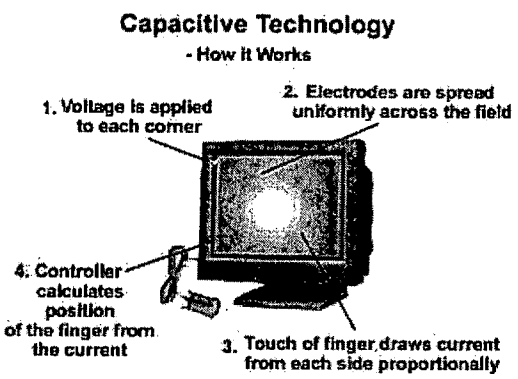

A capacitive touch screen consists of a glass panel with a capacitive (charge storing) material coating its surface. Circuits located at corners of the screen measure the capacitance of a person touching the overlay. Frequency changes are measured to determine the X and Y coordinates of the touch event.

Capacitive type touch screens are very durable, and have a high clarity. They are used in a wide range of applications, from restaurant and POS use to industrial controls and information kiosks.

Advantages

- High touch resolution
- High image clarity
- Not affected by dirt, grease, moisture.

Disadvantages

- Must be touched by finger, will not work with any non-conductive input

Touchscreen Specifications

Touch Type:	3M ClearTek Capacitive
Cable Interface:	PC Serial/COM Port (9-pin) or USB Port
Touch Resolution:	1024 x 1024
Activation Force:	less than 3 ounces
Light Transmission:	88% at 550 nm wavelength (visible light spectrum)
Durability Test:	100,000,000 plus touches at one point
Temperature:	Operating: -15°C to 50°C Storage: -50°C to 85°C
Humidity:	Operating: 90% RH at max 40°C, non-condensing
Chemical Resistance:	The active area of the touchscreen is resistant to all chemicals that do not affect glass, such as: Acetone, Toluene, Methyl ethyl ketone, Isopropyl alcohol, Methyl alcohol, Ethyl acetate, Ammonia-based glass cleaners, Gasoline, Kerosene, Vinegar
Regulations:	UL, CE, TUV, FCC-B
Software Drivers:	Windows XP, 2000, NT, ME, 98, 95, 3.1, DOS, Macintosh OS, Linux, Unix (3rd Party)

A Switched-Capacitor Interface for Capacitive Pressure Sensors

Mitsuhiro Yamada, Takashi Takebayashi, Shun-Ichi Notoyama, and Kenzo Watanabe, *Senior Member, IEEE*

***Abstract*—A switched-capacitor interface for a capacitive pressure sensor is developed which provides a linear digital output. It consists basically of a sample/hold circuit followed by a charge-balancing analog-to-digital converter. The sensor capacitance changes hyperbolically with an applied pressure. To convert the nonlinear capacitance change into the linear digital output, two linearization methods are investigated. In either method, a linear digital output with an accuracy higher than 8-bit is obtained. Because of high accuracy capability and compatible fabrication process, the interface described is best suited for a smart silicon capacitive pressure sensor.**

I. Introduction

ACCORDING to a 1989 survey, pressure sensors get a 60% share of the sensor market. This big market, whose annual sales are now over one billion dollars, was already expected in the late sixties for vast applications in pneumatics, medicine, and automobiles. These applications require low cost, mass producible pressure sensors [1]. To meet such a requirement, the integrated sensor consisting of the piezoresistance bridge diffused or ion implanted onto a silicon diaphragm has been developed [2], [3]. This type of pressure sensor features a good linearity, but suffers from the temperature dependence and large power dissipation.

Lower temperature dependence and small power operation can be expected from capacitive pressure sensors [4], [5]. In addition, their sensitivity is 10 to 20 times higher than that of the piezoresistance bridge [6]. However, the measured capacitance change, which is still small compared to the offset capacitance, is comparable with stray capacitances due to packaging and leads. This makes it mandatory to include interface electronics on the sensor chip.

As an interface to meet this requirement, relaxation oscillators were proposed [7]–[9]. These circuits are simple enough to be fabricated by a CMOS process which is compatible with a capacitive pressure sensor. High resolution cannot be expected, however, because they convert the total capacitance of the sensor into frequency. Another promising candidate for the on-chip interface is the switched-capacitor circuit. Of several such interfaces [10]–[12], those based on the charge-balancing or oversampling principles will be best suited for the capacitive sensor, because offset capacitance cancellation and digital encoding of capacitance change can be realized with a minimum device count [13], [14].

The response of the capacitive pressure sensor is highly nonlinear. This poses another problem to the on-chip interface. This paper endeavors to provide the linearization function in the interface circuit. To this aim, nonlinear behavior of a capacitive pressure sensor is first examined. From this examination, it is concluded that linearization is possible only with digital techniques. As a result, the interface must include the digital encoding function. A switched-capacitor charge-balancing analog-to-digital (A/D) converter is adopted for this application based on work done by [13]. Two approaches to linearization appropriate for the charge-balancing A/D converter are then investigated. In either approach, satisfactory results from prototype interfaces are obtained.

Manuscript received May 14, 1991; revised September 18, 1991.

M. Yamada and K. Watanabe are with the Research Institute of Electronics, Shizuoka University, Hamamatsu, 432 Japan.

T. Takebayashi and S. Notoyama are with the Product Development Department, SMC Corporation, Soka, 340 Japan.

IEEE Log Number 9105796.

II. Electrical Model of Capacitive Pressure Sensors

A general structure of a capacitive pressure sensor is shown in Fig. 1. When the diaphragm, which is anodically bonded to a glass or silicon substrate, bends due to a pressure, the capacitance of a chamber changes.

Assuming a circular diaphragm with the geometric dimensions shown in Fig. 1, the elastic deflection of the diaphragm restrained around its circumference under the pressure P is given by

$$d(r) = \frac{3}{16} P \cdot \frac{1-\mu^2}{Eh^3} R^4 \left\{ 1 - \left(\frac{r}{R} \right)^2 \right\}^2 \tag{1}$$

where h, μ, and E are the thickness, the Poisson ratio, and the elastic modulus of the diaphragm, respectively. The capacitance of the chamber is then expressed by the following integral:

$$C(P) = \epsilon_0 \epsilon_r \int_0^R \frac{2\pi r \, dr}{d_0 - d(r)}. \tag{2}$$

Performing the integral and some manipulation, we can express the capacitance as a function of the fractional pressure x:

$$C(x) = C_0 \frac{1}{\sqrt{x}} \tan h^{-1} \sqrt{x}, \tag{3}$$

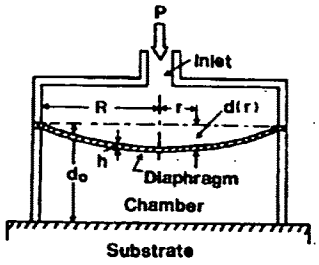

Fig. 1. A structure of a capacitive pressure sensor.

where

$$x = \frac{P}{P_m} (\leq 1), \tag{4}$$

$$P_m = \frac{16}{3} \cdot \frac{E}{1-\mu^2} \cdot \frac{h^3 d_0}{R^4}, \tag{5}$$

and

$$C_0 = \frac{\pi R^2 \epsilon_0 \epsilon_r}{d_0}. \tag{6}$$

It is clear physically that P_m is the maximum allowed pressure which causes a center deflection equal to the chamber depth d_0, and C_0 is the offset capacitance when $P = 0$. Expanding (3) into a Taylor series, we have

$$C(x) = C_0 \sum_{n=0}^{\infty} \frac{x^n}{2n+1}$$

$$\cong C_0 \frac{1-(2/3)x}{1-x} + O(x^2), \tag{7}$$

where $O(x^2)$ denotes the residual term of second-order small.

Some of the practical sensors use stepped diaphragms to increase a pressure sensitivity, and some use square diaphragms fabricated by anisotropic etching techniques. Despite these different structures, it is found experimentally that their capacitance versus pressure characteristics are hyperbolic and can be described by

$$C(x) = C_0 \frac{1-\alpha x}{1-x} = C_0 + \Delta C(x) \tag{8}$$

where

$$\Delta C(x) = C_0 \frac{1-\alpha}{1-x} x. \tag{9}$$

Fig. 2 compares the capacitances measured and approximated by (8) for three capacitive pressure sensors. The parameters α and P_m of each sensor are determined by the measured capacitances. Error between the measured and approximated values is less than 1%. Therefore, a capacitive pressure sensor can be regarded reasonably as a nonlinear capacitor described by (8).

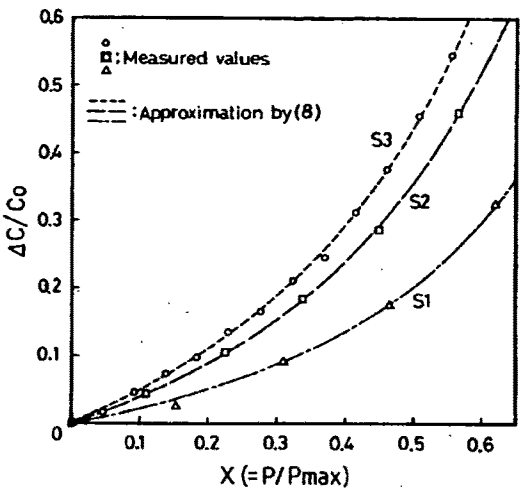

Fig. 2. Capacitance change of diaphragm sensors as a function of applied pressure.

III. Interface

A basic configuration of the interface circuitry is shown in Fig. 3. Here, $C(x)$ denotes the sensor capacitance. The circuit operation is divided into the sample and hold states. In the sample state, the sample/hold (S/H) stage senses the sensor capacitance to its proportional charge $Q(x)$. During the subsequent hold state, the differential integrator (DI) and the comparator (CP) quantize the charge $Q(x)$ held by the S/H stage with respect to the reference charge Q_r. The principle of quantization is based on the charge balance. The counter (CNT) stores the quantized result. Each block will be next described in more detail.

Fig. 4 shows the circuit diagram of the S/H stage. Here, ϕ and $\bar{\phi}$ are the nonoverlapping two phase clocks, ϕ_S and ϕ_H are the state signals discriminating between the sample and hold states, and V_r is a reference voltage. In the ϕ = "1" phase of the sample (ϕ_S = "1") state, the sensor capacitance is charged to the voltage V_r. In the next $\bar{\phi}$ = "1" phase, the charge amplifier formed by op-amp A_1 transfers the charge $Q(x)$ (= $C(x)V_r$) stored in $C(x)$ into the capacitor C_s, producing the output voltage

$$V_0(x) = -Q(x)/C_s. \tag{10}$$

This voltage is stored in the hold capacitor C_h.

During the subsequent hold state when ϕ_H = "1", the capacitor C_h is connected between the virtual ground node ⓐ and the output terminal of op-amp A_1. The hold circuit feeds the charge $C_s V_0(x)$ to the differential integrator (DI) through the node ⓑ every $\bar{\phi}$ = "1" phase. It is noted that the above operation is insensitive to the offset voltage of op-amp A_1 and parasitic capacitances between each node and ground [15], because the offset voltage is canceled by that stored in C_p, and parasitic capacitances are switched between the voltage sources and ground. Fur-

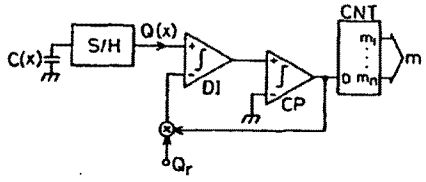

Fig. 3. A block diagram of the interface.

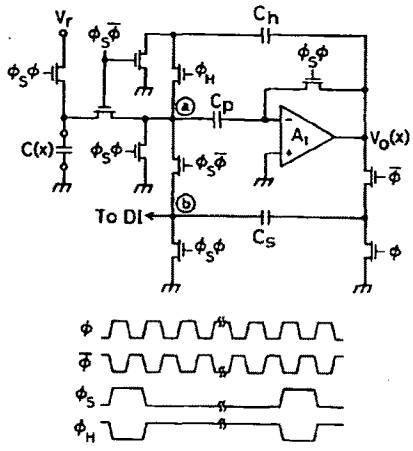

Fig. 4. A circuit diagram of the S/H stage.

thermore, the charge fed to the differential integrator is independent of C_x and C_h.

The circuit diagram of the differential integrator and the comparator is shown in Fig. 5(a). The integrator formed by op-amp A_2 deposits the signal charge $Q(x)$ sent from the S/H stage into the feedback capacitor C_f every $\bar{\phi}$ = "1" phase while extracting the charge $C_c V_c$ concurrently. Thus, if V_c is adjusted such that $C_c V_c$ be equal to the offset charge $C_0 V_r$ stored in $C(x)$, it operates as the charge circuit to accumulate only the charge produced by an applied pressure into C_f. When the accumulated charge reaches the reference voltage $Q_r (= C_r V_r)$, the comparator issues the control signal ϕ_C for the integrator to extract Q_r from C_f. Repeating this process of charge accumulation and extraction for 2^n cycles of the two-phase clock, as shown in the timing diagram of Fig. 5(b), the interface counts ϕ_C using the n-bit counter. The count m at the end of the hold state then represents the capacitance change of the sensor quantized by the reference capacitor C_r:

$$\frac{m}{2^n} = m_1 2^{-1} + m_2 2^{-2} + \cdots + m_n 2^{-n} = \frac{\Delta C(x)}{C_r}. \quad (11)$$

The quantizing process is insensitive again to the offset voltages of op-amp A_2 and comparator, and also to parasitic capacitances. The finite gain of op-amp A_2 has no effect on the quantization, either.

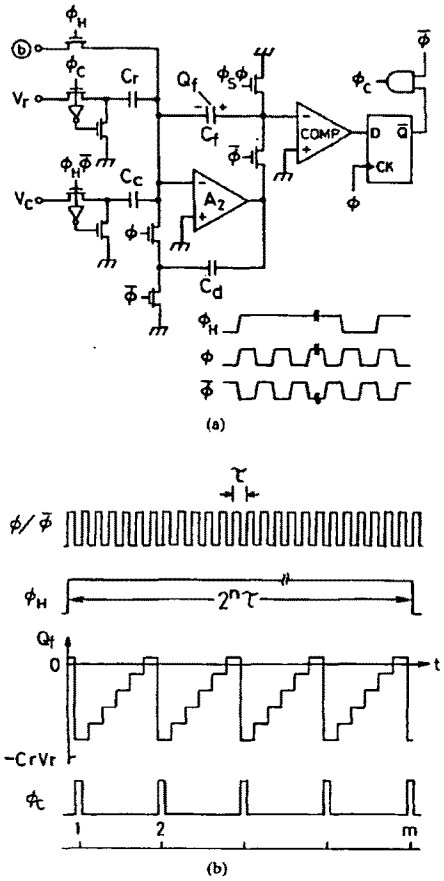

Fig. 5. A circuit diagram of the differential integrator and the comparator (a) and timing diagram of control signals (b).

IV. Linearization

The above-mentioned basic interface converts the capacitance change of the pressure sensor linearly into the digital number. The sensor capacitance changes hyperbolically with a pressure, as described in Section II. Therefore, for the interface to provide the digital output linearly proportional to a pressure, some linearization scheme should be incorporated into the basic configuration.

A well-known circuit technique to linearize a nonlinear sensor is to combine it with a passive linear network. The best approximation to the linear response is then obtained by choosing those circuit parameters of the passive network which make the second derivative of the resultant response as small as possible. This analog technique is not applicable to a capacitive pressure sensor, however, because no inflection point exists in the capacitive versus pressure characteristics. This is evident also by the fact that the capacitance sensitivity, defined as the ratio of the

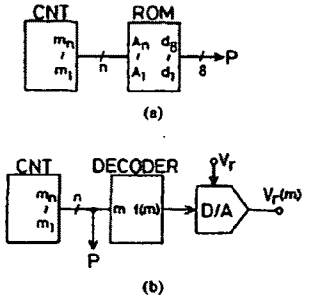

Fig. 6. Table look-up (a) and nonlinear encoding (b) schemes for linearization.

relative change in capacitance to the relative change in pressure, which measures a nonlinearity, is invariant to a linear transformation. Therefore, linearization is possible only with a digital technique. Two such methods are shown in Fig. 6.

(a) Table look-up method: Storing the conversion table in the ROM and addressing it by the m-b counter in the basic configuration, one can get the digital equivalent of the pressure under measurement. Data $D(m)$ stored in the address m is obtained by (9) and (11):

$$D(m) = \frac{m/2}{1 - \alpha + m/2^n} \qquad (m = 0, 1, 2, \cdots, 2^n - 1). \quad (12)$$

A resolution required in most pressure measurements is 1%, and thus 8 b is enough for the word length. The table address size is determined by the measurement range as follows.

The sensitivity of the capacitance change to the fractional pressure is given by

$$S_x^{\Delta C(x)} = \frac{\partial \ln \Delta C(x)}{\partial \ln x} = \frac{1}{1 - x}. \quad (13)$$

Assume now the fractional pressure in the range from 0 to 3/4 is to be measured. The sensitivity in the lower bound ($x \to 0$) is 1. This implies that the capacitance, and hence m, increases linearly with a pressure. The sensitivity in the upper bound, on the other hand, is 4. Therefore, the table address size should be four times larger than the word length; i.e., 1% resolution over the range quoted above requires the address size 10-b wide. This is not a serious problem to the interface because it allows a higher accuracy A/D conversion, but a low sampling rate is inevitable.

(b) Nonlinear coding method: Referring to the charge balance condition, $2^n Q(x) = mQ_r$, involved in the basic interface configuration, one notices that not the capacitance but the pressure can be linearly encoded by changing the reference charge Q_r in a manner similar to $Q(x)$. Since the output m is then the digital equivalent of x, this is accomplished by decoding m, as shown in Fig. 6(b). The decoder function $f(m)$ can be derived from (9):

$$f(m) = \frac{1 - \alpha}{(1 - m)^2}. \quad (14)$$

This method of linearization requires a D/A converter. Thus, reducing the decoder size is crucial. A technique useful for the reduction is to divide the decoder function $f(m)$ into segments by a piecewise linear approximation. A 1% resolution can be achieved usually by 32 segments or less. The input m to the decoder is the digital equivalent of the pressure under measurement, and thus 8 b is enough for most applications. Compared to the table look-up method, this method requires a larger device count, but allows a higher sampling rate.

V. Experimental Results

Prototype interfaces were built using discrete components. Op-amp and switches used are LF356 and MC14016, respectively. The clock frequency is 10 kHz. Other circuit parameters are: $V_r = 5$ V, $C_i = 1$ nF, $C_h = 3.9$ nF, $C_r = 102.2$ pF, $C_f = 1.5$ nF, and $C_d = 1.5$ nF. The capacitive pressure sensor numbered S2 in Fig. 2 is used. Its offset capacitance C_0 is 50 pF. The parameters α and P_m calculated using the measured capacitance are 0.64 and 3.56 kgf/cm^2, respectively. The pressure applied to the sensor by means of a compressor was measured by a commercially available manometer. The measurement accuracy is $\pm 0.1\%$ of the 10 kgf/cm^2 FS.

Data stored in the look-up table is shown in Fig. 7(a) as a function of the address m. The area below the address 65 is saved for the offset capacitance C_0. The table size is 4 k ($= 2^{12}$) $\times$ 8b. The sampling rate is thus about 2.5 sample-per-second (sps). Fig. 7(b) compares the digital output of the prototype interface displayed on seven-segment LED's with the reading of the commercial manometer. Error between them is less than 1%.

The decoding function $f(m)$ for the nonlinear encoding was divided into 32 segments and stored into a ROM in table form for easy implementation. Data $f(m)$ stored in the table is plotted in Fig. 8(a) as a function of the address m. The table size is 256 ($= 2^8$) $\times$ 5b. The clock frequency is reduced to 7.68 kHz, and thus the sampling rate is 30 sps. The 5-b D/A converter was built using an R-2R ladder. The pressure displayed by the prototype interface is compared with the reading of the commercial manometer in Fig. 8(b). Both are in good agreement except for the lower and upper bounds, and error between them is within 1%.

VI. Conclusions

An interface circuit for a capacitive pressure sensor based on the switched-capacitor charge-balancing A/D converter and two linearization techniques were described. Prototype interfaces built using discrete components were also presented to demonstrate the validity of

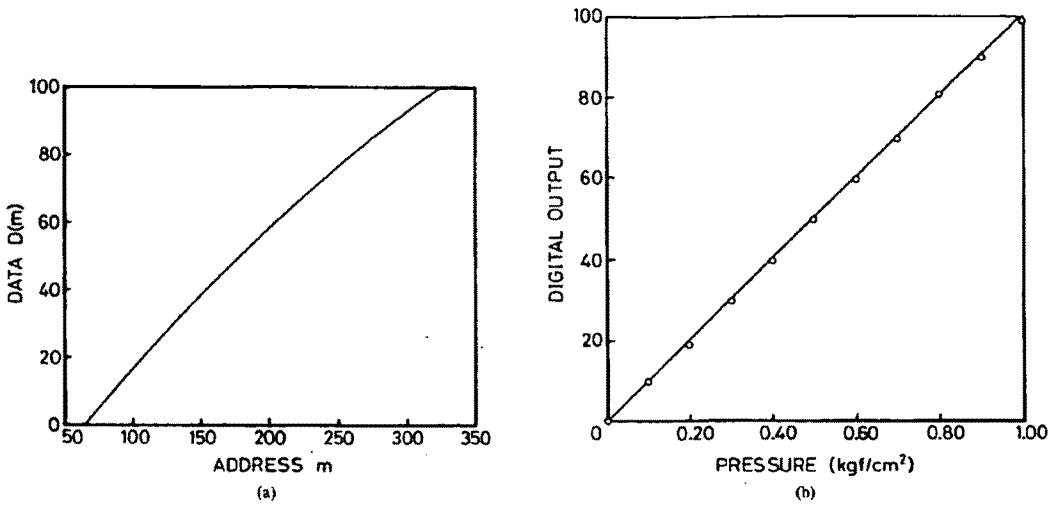

Fig. 7. Data $D(m)$ stored in the look-up table (a) and the digital output of a prototype interface compared with the reading of a commercial manometer (b).

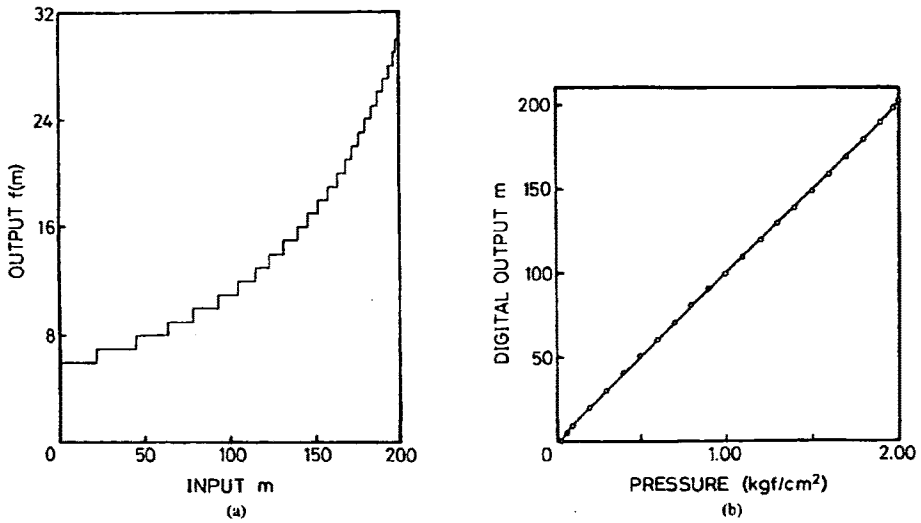

Fig. 8. The decoder output $f(m)$ stored in a ROM in table form (a) and the digital reading displayed by a prototype interface compared with that of a commercial manometer (b).

the linearization approaches. In realizing the nonlinear encoding approach, the D/A converter using an R-2R ladder was used. Replacing it by a switched-capacitor array will facilitate the monolithic implementation of the interface. This is a future work.

Though different in structure, a great many humidity, displacement, thickness, and flow sensors detect the measurands by their capacitance changes. The interface described herein will find wide applicability in these capacitive sensors, since it meets such requirements as the on-chip implementation, digital output, high sensitivity, and good linearity.

References

[1] S. Middlehoek and S. A. Audet, *Silicon Sensors*. London: Academic Press, 1989, chap. 3.
[2] Samaun, K. D. Wise, and J. B. Angell, "An IC piezoresistive pres-

sure sensor for biomedical instrumentation," *IEEE Trans. Biomed. Eng.*, vol. BME-20, pp. 101-109, March 1973.
[3] S. Sugiyama, M. Takigawa, and I. Igarashi, "Integrated piezoresistive pressure sensor with both voltage and frequency outputs," *Sensors and Actuators*, vol. 4, pp. 113-120, 1983.
[4] Y. S. Lee and K. D. Wise, "A batch-fabricated silicon capacitive pressure sensor with low temperature sensitivity," *IEEE Trans. Electron Devices*, vol. ED-29, pp. 42-48, Jan. 1982.
[5] W. H. Ko, "Solid-state capacitive pressure transducers," *Sensors and Actuators*, vol. 10, pp. 303-320, 1986.
[6] S. K. Clark and K. D. Wise, "Pressure sensitivity in anisotropically etched thin-diaphragm pressure sensors," *IEEE Trans. Electron Devices*, vol. ED-26, pp. 1887-1896, Dec. 1979.
[7] A. Hanneborg, T. E. Hansen, P. A. Ohlckers, E. Carlson, B. Dahl, and O. Holweck, "An integrated capacitive pressure sensors with frequency modulated output," *Sensors and Actuators*, vol. 9, pp. 345-351, 1986.
[8] J. Neumeister, G. Shuster, and W. von Munch, "A silicon pressure sensor using MOS ring oscillators," *Sensors and Actuators*, vol. 7, pp. 167-176, 1985.
[9] M. Esashi, S. Shoji, T. Wada, and T. Nagata, "Capacitive absolute pressure sensors with hybrid structure," (in Japanese) *Trans. IEICE*, vol. J73-CII, pp. 461-467, Aug. 1990.
[10] Y. E. Park and K. D. Wise, "An MOS switched-capacitor readout amplifier for capacitive pressure sensors," in *Proc. Custom Integrated Circuits Conf.*, 1983, pp. 380-384.
[11] E. Habekotte and S. Cserveny, "A smart digital-readout circuit for a capacitive microtransducers," *IEEE Micro*, pp. 44-54, Oct. 1984.
[12] G. J. Yeh, I. Dendo, and W. H. Ko, "Switched-capacitor interface circuit for capacitive transducers," in *Dig. Int. Conf. Solid-State Sensors and Actuators*, 1985, pp. 60-63.
[13] H. Matsumoto, H. Shimizu, and K. Watanabe, "A switched-capacitor charge-balancing analog-to-digital converter and its application to capacitance measurement," *IEEE Trans. Instrum. Meas.*, vol. IM-36, pp. 873-878, Dec. 1987.
[14] A. Cichocki and R. Unbehauen, "Application of switched-capacitor self-oscillating circuits to the conversion of RLC parameters into a frequency or digital signal," *Sensors and Actuators A*, vol. 24, pp. 129-137, 1990.
[15] K. Nagaraj, J. Vlach, T. R. Viswanathan, and K. Singhal, "Switched-capacitor integrator with reduced sensitivity to amplifier gain," *Electron. Lett.*, vol. 22, pp. 1103-1105, 1986.

The DigitalDesk Calculator: Tangible Manipulation on a Desk Top Display

Pierre Wellner

University of Cambridge Computer Laboratory
and
Rank Xerox EuroPARC
61 Regent Street
Cambridge CB2 1AB (United Kingdom)
Wellner@EuroPARC.Xerox.COM

Abstract

Today's electronic desktop is quite separate from the physical desk of the user. Electronic documents lack many useful properties of paper, and paper lacks useful properties of electronic documents. Instead of making the electronic desktop more like the physical desk, this work attempts the opposite: to give the physical desk electronic properties and merge the two desktops into one. This paper describes a desk with a computer-controlled camera and projector above it. The camera sees where the user is pointing, and it reads portions of documents that are placed on the desk. The projector displays feedback and electronic objects onto the desk surface. This DigitalDesk adds electronic features to physical paper, and it adds physical features to electronic documents. The system allows the user to interact with paper and electronic objects by *touching* them with a bare finger (digit). Instead of "direct" manipulation with a mouse, this is *tangible* manipulation with a finger. The DigitalDesk Calculator is a prototype example of a simple application that can benefit from the interaction techniques enabled by this desktop. The paper begins by discussing the motivation behind this work, then describes the DigitalDesk, tangible manipulation, and the calculator prototype. It then discusses implementation details and ends with ideas for the future of tangible manipulation.

Keywords: user interface, interaction technique, display, input device, workstation, desk, desktop.

Introduction

Many of us work at a desk, and an important part of desk activities involve "paper pushing," or the manipulation of paper documents. Although paperwork on the desk and electronic work on the workstation are often related, the two activities are quite distinct. Interaction techniques in the two environments are very different, and mastering one does not help master the other. Given the amount of time we spend at work, the quality of this desk interface makes up an important element in our quality of life. The conventional outlook for computerized desktops is that personal workstations are destined to evolve into faster machines with integrated 3D graphics and full-motion audio/video. More and more functionality is expected to migrate onto these super-workstations and off the conventional paper pusher's desktop. This paper presents an alternative.

Advances in digital technology are enabling computers to sense and synthesize many aspects of our environment. This has been exploited in the field of human-computer interaction (HCI) primarily through the study of virtual reality (VR), where users can interact with completely synthesized worlds using, for example, 3D head-mounted displays and data gloves [Spri91]. Even the traditional workstation is a limited sort of virtual reality, where the world resembles a desk work surface adorned with windows, icons and menus.

Computerized reality

But what about the *real* world? Some computer applications exploit the familiar world, not by simulating it electronically, but by enhancing it. Instead of virtual reality, these systems create *computerized* reality (CR). Users do not have

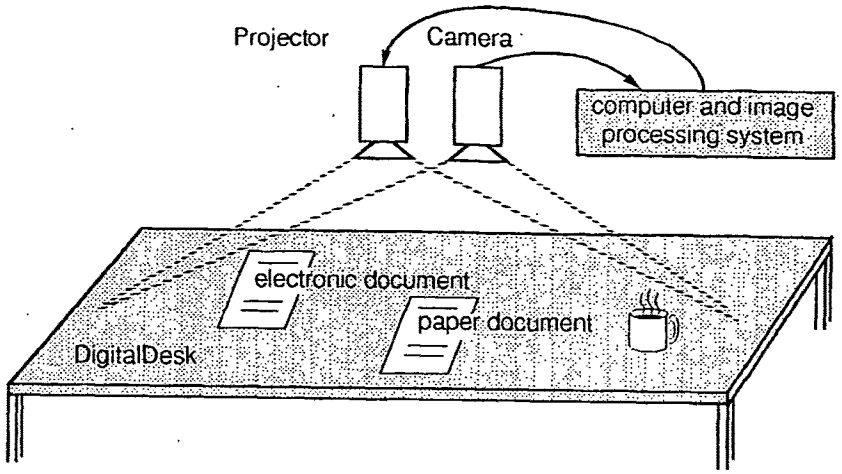

Figure 1. A DigitalDesk system

to enter a new world to use these systems. Instead, they continue to interact with familiar objects almost as before, but the computer adds new functionality.

Many existing systems are examples of computerized reality. At the University of Cambridge Computer Laboratory and Rank Xerox EuroPARC, for example, several systems use Active Badges [Want90] to detect peoples' movements throughout the buildings: Pepys [Newm91a] automatically creates a diary of daily activities for badge wearers, and BirdDog [OShe91] changes its display depending on who is in the room. The rooms in these buildings have added functionality without requiring people to use them differently. Other devices that preserve a familiar interface while enhancing it with electronic features are musical instruments such as computerized keyboards, guitars and drums. Head-up displays [Wein91] create CR because instead of *replacing* what the user sees, they enhance it by superimposing a computer-generated image onto the real world. This approach to HCI has great advantages over the VR approach. Familiar tools are still usable as before, because CR interfaces are designed to be upwardly compatible with our interfaces to ordinary real-world objects. More examples of CR being developed at Xerox PARC are described in [Weis91].

Today's workstation requires the user to abandon the familiarity of the physical desk and enter the virtual world of the electronic desktop. Instead of VR, this paper applies CR to the desk. It describes a prototype DigitalDesk which attempts to merge the physical and electronic desktops into one. It does not use the desktop *metaphor* because it is *literally* a desk top. With this desk, we can begin to explore interaction techniques that could significantly change the way users interact with and think about computerized desktops.

The DigitalDesk

The DigitalDesk is an ordinary desk and can be used as such, but it has a few extra capabilities. A video camera is mounted above the desk pointing down at the work surface. This camera's output is fed through a system that can detect where the user is pointing, and it can read portions of documents that are placed on the desk. A computer-driven projector is also mounted above the desk, allowing the system to superimpose electronic objects onto paper documents and the user's work surface [See Figure 1].

This system shares some features of the VIDEODESK, by Myron Krueger [Krue83, Krue84]. Krueger's system consists of a light table with a video camera pointing down on it. Behind the table is a screen with the user's silhouette and various graphical objects that the user can interact with. The Mandala system [Vinc90] also uses a video camera to let a person control a musical performance using his or her entire body instead of just the hands. The DigitalDesk differs from these systems in that feedback is projected back onto the desk instead of on a separate screen. Another difference is

that the camera is not only used to detect the position of the hands, but also to read portions of documents. The following sections describe the three key features of a DigitalDesk: using a camera to allow pointing with the fingers, reading paper documents on the desk, and projecting images onto the desk.

Using a camera to allow pointing with the fingers

The DigitalDesk aims to make electronic interactions on the desktop nearly identical to physical interactions. This requires manipulating objects with unencumbered hands, requiring an input technique such as image-based hand tracking. There are several problems with this approach to hand tracking [Stur91], but they fall into two main categories: performance limitations and occlusion. The performance problems are being solved as computer hardware improves, and occlusion of the fingers (by other objects and parts of the body) does not seem to be a significant problem in the context of desk work. Hands on a desk have a limited range of motion, and desk work is mainly two dimensional. Pointing at things on the DigitalDesk is much like pointing out things to another person. The finger works well when pointing to large objects, but for higher precision, as when pointing to a single character, it is useful to point with something like a pen to avoid ambiguity. The current implementation only allows a single pointer, but Krueger's VIDEODESK demonstrated a wide variety of additional single and multi-finger interaction techniques that could also be used.

A problem when observing the hands through an overhead camera is that it is difficult to determine exactly the moment when the user presses something. A pause in movement often occurs without a press being intended. This problem is solved relatively easily, however, by listening. A small snare-drum microphone is attached underneath the desk and its digitized signal is fed into the system. From this data, the system detects a tap. A more difficult problem is how to detect dragging. More sophisticated sound processing could be used or a second camera, but the easiest solution seems to be placing a touch pad in the surface of the desk. From a CR point of view, a digitizing tablet is not as effective in merging the electronic and physical desktops because it requires holding a special-purpose pointing device. The basic finger-following system can be used as an alternative pointing device for a conventional workstation, but the DigitalDesk does more than this.

Because the DigitalDesk needs to read documents in addition to tracking the hand, it cannot rely on having a bright white background, as VIDEODESK and the Mandala system do. It must be able to distinguish the hand from documents and clutter appearing on the desk. The main distinguishing characteristic of hands is that they move, so finger-following is currently accomplished by using image differencing to perform motion detection. Although changes in the image occur for other reasons than moving hands, this technique is reasonably accurate.

Reading portions of documents on the desk

A great deal of information comes to us as printed matter. The "paperless office" predicted in the 70's never happened. In fact, the market for business paper has continued to grow faster than the general economy [Xero91]. Paper is cheap, very high resolution, portable, universal, and you can spread it out all over your desk. A computerized desktop ought to be able to access some of this paper-based information electronically. A natural way to input a page or less of text into a computer is to point at the text with a finger. This is how we show text to another person, and it is much simpler than using a scanner, no matter how small. One difficulty is that the finger sometimes obscures some of the characters. Other difficulties, such as poor lighting, are discussed below in the section on implementation issues. A greater problem, however, is the low resolution of standard video cameras. One approach to this problem, taken by a related project at EuroPARC [Newm91b], is to simulate a high resolution camera by manually pre-scanning documents then using the low resolution camera image to look up the corresponding scanned document. This work instead uses multiple cameras, some of which are zoomed in very close to the desk. The system generally looks through a wide angle view to track the finger, but it switches to a close-up view to do character recognition. In the long run, high definition television and advances in cheap, integrated digital cameras will make this approach more practical than it is today.

Projecting images on the desktop

Projection provides similar capabilities to using a large flat display screen, but it has the advantage that computer-generated images can be superimposed on paper documents. A problem with overhead projection is shadows; for example, one cannot lean over to look at a projected image too closely. In practice, however, this has not yet proved to be a problem. Another issue with projection is the brightness of the room. The projector used in these experiments works quite well with the room's normal fluorescent lights, but a bright desk lamp makes the display unreadable. The same would be true of direct sunlight, so this limits the desk's usability in some settings. One last problem with projection is that not all surfaces make good screens. The projection area should be white in order to see the projected images

most clearly. An ideal system would have projection both from above and from below.

Tangible manipulation

A goal of the DigitalDesk is to apply computerized reality to the desk. This means that interactions on the DigitalDesk should be upwardly compatible with interactions on an ordinary desk, *i.e.* the old way should still work. The old way to interact with objects on the desk is to reach out and touch them. On a DigitalDesk, both physical and electronic objects can be manipulated by touching them. This is different from mouse-based "direct" manipulation (which is actually not direct at all). This is *tangible* manipulation. These interfaces are designed to work in the same way for both electronic and physical objects. The goal here is that when the user learns to do something with an electronic document, he or she can do the same thing to a paper document, and vice versa. Although this goal may never be fully achieved, it is the driving spirit of this research.

The DigitalDesk Calculator

The DigitalDesk Calculator is a prototype of a simple example that illustrates how an application might benefit from tangible manipulation. Informal and video-recorded observations [Harp91] indicate that people using desk calculators often enter numbers that are already printed on a piece of paper lying on the desk. Users have to manually copy the numbers into the calculator in order to perform arithmetic on them. Transcribing these numbers can constitute a large proportion of the keystrokes when using a calculator, and a large proportion of the errors.

The DigitalDesk Calculator is projected onto the desktop, and the user can use it much like a regular electronic calculator. The projected cursor follows the user's finger as it moves around on the desktop. To enter a number, the user taps on the desired projected buttons. The advantage of this calculator over an ordinary calculator, however, is that it has an additional way to enter numbers. If the number to be entered is already printed on a piece of paper lying on the desk, the user can simply point at it with a finger or other pointer. In front of the user's finger is projected a rectangle that indicates what is being pointed to. When the user taps, the system reads the number with the camera, recognizes it, and treats it as though the digits had been typed into the calculator by hand. Feedback is provided by displaying the indicated numbers in the projected calculator.

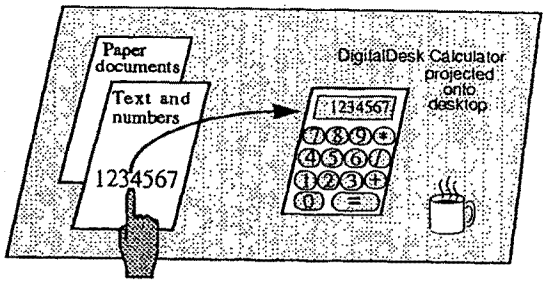

Figure 2. The DigitalDesk calculator

An example where this would be useful is when a price list for a variety of items is on the desk and cost calculations need to be made from these prices. Almost all the relevant numbers are already on the paper and can easily be input using this system. Tangible manipulation is used to physically drag the price list on the desk, and to electronically select the numbers. Much fewer keystrokes are required to perform the calculations than with a conventional calculator.

The current implementation only recognizes a single typeface, and the number must be somewhat isolated from the text. The system is therefore a prototype, not yet robust enough for real users, but it demonstrates the utility of the concept.

Implementation Issues

Processing images in real time

Response time is considered one of the chief determinants of user satisfaction with interactive computer systems [Baec87]. This is especially true for direct manipulation systems, VR systems, and it will also be true for a DigitalDesk. Sophisticated pattern matching algorithms can be used when there are no time limits, but this system should ideally be able to process every video frame, which means processing 25 or 30 frames per second. This requires either very fast special-purpose hardware, or techniques for minimizing the amount of processing required.

The current implementation uses simple image processing hardware. It initially subsamples the image of the desk surface and processes it at very low resolution to get an approximate location for the finger. Only then does the system scale to its full resolution in order to get a precise location, so only small portions of the image need to be

processed. If the user moves too quickly, the system loses track of where the finger is, so it immediately zooms back out to find it. The result is that large, quick movements are followed less precisely than fine movements, but for pointing applications this seems acceptable.

Motion detection uses an image loop-back feature of the image processing board that allows the most significant bits of two images to be sent through a lookup table. This table is set up to subtract the two images, allowing very fast differencing of sequential frames. Current finger-tracking performance using a Sun 4/110 and an Itex100 image processing board is between 6 and 7 frames per second.

Obtaining a high contrast image

Simple thresholding is not adequate for obtaining an image suitable for character or finger recognition. In normal office lighting, the range of brightness on different parts of the desk varies greatly, so a simple threshold creates large patches of black and white. Another problem can be automatic gray balancing on the camera. This can cause a change in brightness in one part of the image to affect the values in all other parts. These problems were solved, however, by using a histogram-based adaptive thresholding method [Wall74, Cast79].

System architecture

One of the goals in this DigitalDesk implementation was to be able to run standard X Window applications using the finger as a pointing device. The system is implemented so that finger location and tapping information are sent through X in such a way that from the point of view of applications, these events are indistinguishable from those of the mouse. The system runs on two machines: a Sun 4/110 and a SPARCstation. This is because the image processing board plugs into a VME bus, while the projected LCD display plugs into an Sbus. Figure 3 illustrates how the software modules interface to each other and the hardware (note key in the bottom right corner). The system is implemented in C++ and C under SunOS and TCP/IP.

Future Tangible Manipulation

The currently implemented DigitalDesk has only begun to explore the possibilities for tangible manipulation. This section describes some additional ways in which a DigitalDesk could be used. Although not yet currently implemented, the following examples illustrate the style of interaction that tangible manipulation might enable in the future.

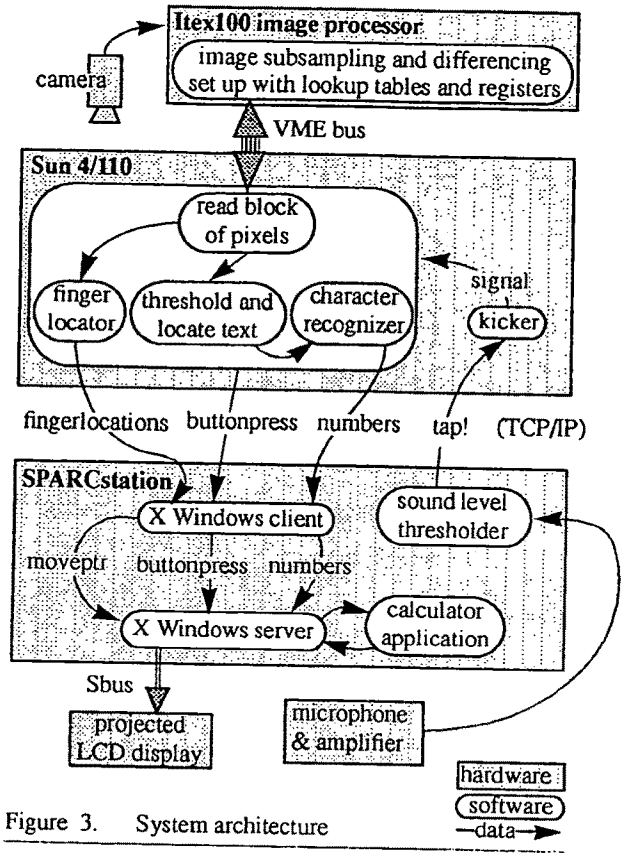

Figure 3. System architecture

Medium-independent tools

Fingers are not the only things that can be used in both the electronic and physical medium on a DigitalDesk. Conventional desk tools can also benefit from being computerized when they are used on this desk if the tools are recognized by the system. An ordinary eraser, for example, can be made to erase electronic documents in addition to physical documents. A stapler could be used to attach electronic documents together, and a staple remover would detach them.

Moving between the paper and electronic worlds

Both electronic and paper documents can be dragged on the surface of a DigitalDesk with the hands. In order to further integrate the two sides of the desk it would be useful to have a "door" between them. This can be implemented with two slots on the side of the desktop. If the user drags an electronic document to one of the slots (a printer), then it comes out as a paper document. If the user drags a paper document to the other slot (a scanner), then it enters the desk as an

electronic document. It may be possible to implement this with a single slot: why have a separate in-door and out-door? In Figure 4, the solid arrows indicate movements of documents by hand.

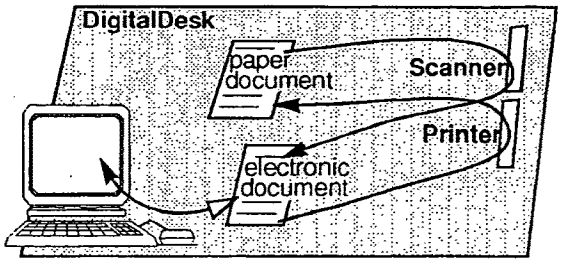

Figure 4. Moving documents through the desktop

This desktop could replace a conventional workstation, but some users may want to remain backward-compatible with the workstation style of interaction. The two can be integrated by allowing the user to drag electronic documents into the workstation by hand, and out of the workstation by mouse.

The mode of use thus encouraged by this system is for users to continuously move documents back and forth between the physical and electronic media, and to work on a document in both places, depending on which medium seems better suited to the particular task. Ideally, the user should hardly be aware of where the document is. The physical and electronic desktops complement and enhance each other.

Conclusion

Today's electronic desktop is a kind of "virtual reality," quite separate from the physical desk of the user. A "computerized reality" approach to HCI, on the other hand, seeks to add computer functionality to physical objects and environments while allowing people to continue interacting with them as before. The DigitalDesk applies this approach to the desk, and attempts to merge the physical world of paper, pens and tape with the electronic world of the workstation. The DigitalDesk Calculator is an example that illustrates how merging these two worlds can improve the usability of a very simple and well-established application. The style of interaction enabled by a digital desk is different than mouse-based "direct manipulation," because users manipulate both electronic and physical objects by *touching* them with their fingers. This style of "tangible manipulation" makes possible new interaction techniques that offer important advantages over currently used techniques, but it does not preclude them. Tangible manipulation on a digital desk brings the desktop back to the desk top, and it offers advantages over conventional workstations that, in some settings, could render them obsolete.

Acknowledgments

Many have contributed inspiration, help getting equipment to work and insightful comments. The following people deserve special mention: Stu Card, Matthew Chalmers, Scott Elrod, Steve Freeman, Nicolas Graube, Austin Henderson, Mik Lamming, Linda Malgeri, Mike Molloy, Tom Moran, William Newman, Peter Robinson, Z Smith and Mark Weiser.

The author is very interested in comments from readers, particularly suggestions for specific applications that seem well suited to this technology.

References

[Baec87] Baecker, R. and Buxton, W. *Readings in Human-Computer Interaction - A Multidisciplinary Approach*, p606. Morgan Kaufmann, Los Altos, California, 1987.

[Cast79] Castleman, K. *Digital Image Processing*. Prentice-Hall Signal Processing Series, 1979.

[Harp91] Harper, R. Internal EuroPARC videotapes of administrative desk work.

[Krue84] Krueger, M. *VIDEOPLACE -- An Artificial Reality*. CHI '84 Proceedings.

[Krue83] Krueger, M. *Artificial Reality*. Addison-Wesley, 1983.

[Newm91a] Newman, W., Eldridge, M. and Lamming, M. *Pepys: Generating Autobiographies by Automatic Tracking*. ECSCW, Amsterdam.

[Newm91b] Newman, W. *Interacting with Paper Documents*. Proceedings of NordDATA '91 June 16-19; Oslo 1991, 107-114.

[OShe91] O'Shea, T., Lamming, M., Chalmers, M., Graube, N., Wellner, P., Wiginton, G. *Expectations and Perceptions of Ubiquitous Computing: Experiments with BirdDog, a prototype Person Locator.* in BCS/IEE ITaP '91.

[Spri91] Spring, M. *Virtual Reality - Theory, Practice, and Promise.* Meckler, 1991.

[Stur91] Sturman, D. J. *Motivations, Applications, and Areas of Study for Whole-hand Input.* Submitted to *Presence*, MIT Press, March 1991.

[Vinc90] Vincent, J. V., MacDougall, F. *The Mandala System*, CHI '90 Interactive experience, April 1-5 1990. Seattle, Washington.

[Wall74] Wall, R.J. *The Gray Level Histogram for Threshold Boundary Determination in Image Processing with Applications to the Scene Segmentation Problem in Human Chromosome Analysis.* Ph.D. Dissertation. University of California at Los Angeles, 1974.

[Want90] Want, R. *The Active Badge Locator System.* Olivetti Research Laboratories, The Old Addenbrooks Site, 24a Trumpington St., Cambridge, CBQ 12N England.

[Wein91] Weintraub, D. J. *Head-Up Displays: A Human Factors Analysis.* CSERIAC Report, in progress 1991.

[Weis91] Weiser, M. *The Computer for the 21st Century.* To appear in Scientific American, September 1991. (In this article, the term "embodied virtuality" is used instead of "computerized reality")

[Xero91] Xerox paper product manager's office, private communication, 26 June 1991.

TSC2003

SBAS162F – NOVEMBER 2000 – REVISED JANUARY 2005

I²C TOUCH SCREEN CONTROLLER

FEATURES

- 2.5V TO 5.25V OPERATION
- INTERNAL 2.5V REFERENCE
- DIRECT BATTERY MEASUREMENT (0.5V TO 6V)
- ON-CHIP TEMPERATURE MEASUREMENT
- TOUCH-PRESSURE MEASUREMENT
- I²C INTERFACE SUPPORTS: Standard, Fast, and High-Speed Modes
- AUTO POWER DOWN
- TSSOP-16 AND VFBGA-48 PACKAGES

APPLICATIONS

- PERSONAL DIGITAL ASSISTANTS
- PORTABLE INSTRUMENTS
- POINT-OF-SALES TERMINALS
- PAGERS
- TOUCH SCREEN MONITORS
- CELLULAR PHONES

DESCRIPTION

The TSC2003 is a 4-wire resistive touch screen controller. It also features direct measurement of two batteries, two auxiliary analog inputs, temperature measurement, and touch-pressure measurement.

The TSC2003 has an on-chip 2.5V reference that can be utilized for the auxiliary inputs, battery monitors, and temperature-measurement modes. The reference can also be powered down when not used to conserve power. The internal reference will operate down to 2.7V supply voltage while monitoring the battery voltage from 0.5V to 6V.

The TSC2003 is available in the small TSSOP-16 and VFBGA-48 packages and is specified over the –40°C to +85°C temperature range.

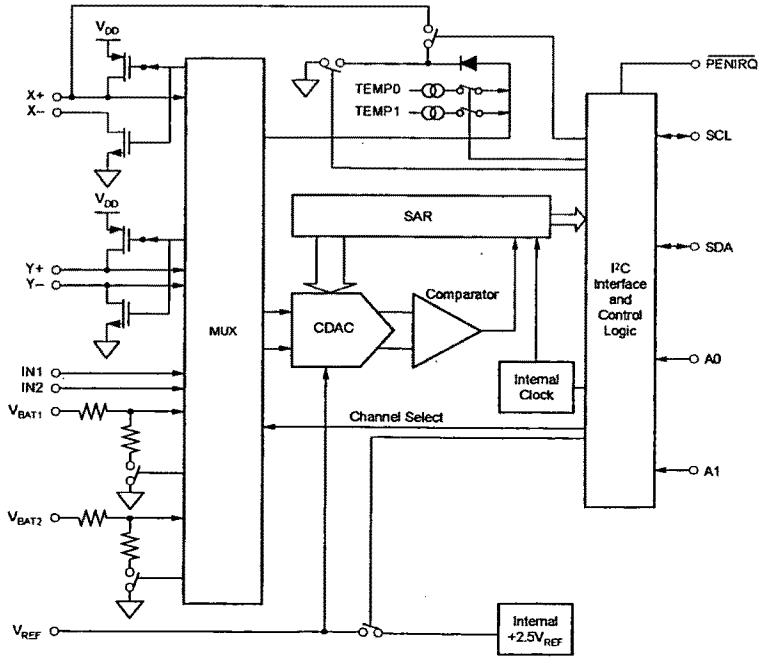

Please be aware that an important notice concerning availability, standard warranty, and use in critical applications of Texas Instruments semiconductor products and disclaimers thereto appears at the end of this data sheet.

PACKAGE/ORDERING INFORMATION[1]

PRODUCT	MAXIMUM RELATIVE ACCURACY (LSB)	MAXIMUM GAIN ERROR (LSB)	PACKAGE-LEAD	PACKAGE DESIGNATOR	SPECIFIED TEMPERATURE RANGE	PACKAGE MARKING	ORDERING NUMBER
TSC2003	±2	±4	TSSOP-16	PW	–40°C to +85°C	TSC2003I	TSC2003IPW
TSC2003	±2	±4	TSSOP-16	PW	–40°C to +85°C	TSC2003I	TSC2003IPWT
TSC2003	±2	±4	TSSOP-16	PW	–40°C to +85°C	TSC2003I	TSC2003IPWR
TSC2003	±2	±4	TSSOP-16	PW	–40°C to +85°C	TSC2003I	TSC2003IPWRG4
TSC2003	±2	±4	VFBGA-48	ZQC	–40°C to +85°C	BC2003	TSC2003IZQCT
TSC2003	±2	±4	VFBGA-48	ZQC	–40°C to +85°C	BC2003	TSC2003IZQCR

NOTE: (1) For the most current package and ordering information, see the Package Option Addendum located at the end of this data sheet, or refer to our web site at www.ti.com.

ELECTROSTATIC DISCHARGE SENSITIVITY

This integrated circuit can be damaged by ESD. Texas Instruments recommends that all integrated circuits be handled with appropriate precautions. Failure to observe proper handling and installation procedures can cause damage.

ESD damage can range from subtle performance degradation to complete device failure. Precision integrated circuits may be more susceptible to damage because very small parametric changes could cause the device not to meet its published specifications.

PIN CONFIGURATION

Top View TSSOP

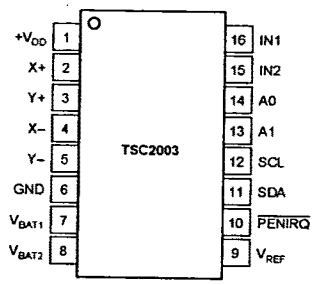

Top View VFBGA

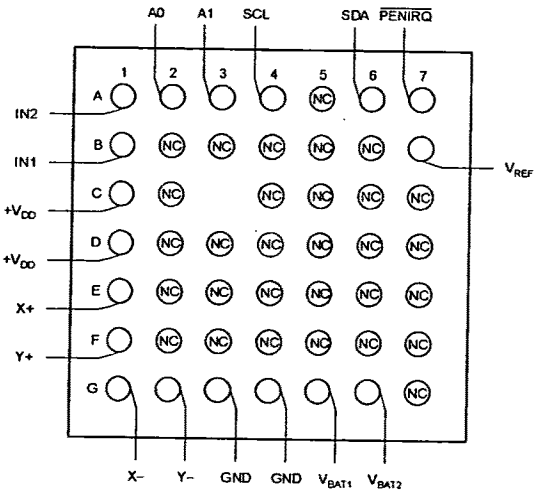

NC = No Connection

ABSOLUTE MAXIMUM RATINGS[1]

$+V_{DD}$ to GND	–0.3V to +6V
Digital Input Voltage to GND	–0.3V to $+V_{DD}$ + 0.3V
Analog Input Voltage to GND. All Pins Except 7, 8	–0.3V to $+V_{DD}$ + 0.3V
Analog Input Voltage Pins 7, 8 to GND	–0.3V to +6.0V
Operating Temperature Range	–40°C to +85°C
Storage Temperature Range	–65°C to +150°C
Power Dissipation	$(T_J$ Max – $T_A)/\theta_{JA}$
TSSOP Package	
Junction Temperature (T_J Max)	+150°C
θ_{JA} Thermal Impedance	+115.2°C/W
Lead Temperature, Soldering	
Vapor Phase (60s)	+215°C
Infrared (15s)	+220°C
VFBGA Package	
Junction Temperature (T_J Max)	+125°C
θ_{JA} Thermal Impedance	+50°C/W
Lead Temperature, Soldering	
Vapor Phase (60s)	+215°C
Infrared (15s)	+220°C

NOTE: (1) Stresses above those listed under *Absolute Maximum Ratings* may cause permanent damage to the device. Exposure to absolute maximum conditions for extended periods may affect device reliability.

PIN DESCRIPTIONS

TSSOP PIN #	VFBGA PIN #	NAME	DESCRIPTION
1	C1, D1	$+V_{DD}$	Power Supply
2	E1	X+	X+ Position Input
3	F1	Y+	Y+ Position Input
4	G1	X–	X– Position Input
5	G2	Y–	Y– Position Input
6	G3, G4	GND	Ground
7	G5	V_{BAT1}	Battery Monitor Input
8	G6	V_{BAT2}	Battery Monitor Input
9	B7	V_{REF}	Voltage Reference Input/Output
10	A7	$\overline{PENIRQ}$	Pen Interrupt. Open Drain Output (Requires 30kΩ to 100kΩ pull-up resistor externally).
11	A6	SDA	Serial Data
12	A4	SCL	Serial Clock
13	A3	A1	I^2C Bus Address Input A1
14	A2	A0	I^2C Bus Address Input A0
15	A1	IN2	Auxiliary A/D Converter Input
16	B1	IN1	Auxiliary A/D Converter Input

ELECTRICAL CHARACTERISTICS

At T_A = –40°C to +85°C, $+V_{DD}$ = +2.7V, V_{REF} = 2.5V external voltage, I²C bus frequency = 3.4MHz, 12-bit mode and digital inputs = GND or $+V_{DD}$, unless otherwise noted.

PARAMETER	CONDITIONS	TSC2003I			
		MIN	TYP	MAX	UNITS
ANALOG INPUT					
Full-Scale Input Span		0		V_{REF}	V
Absolute Input Range		–0.2		$+V_{DD}$ +0.2	V
Capacitance			25		pF
Leakage Current			0.1		µA
SYSTEM PERFORMANCE					
Resolution			12		Bits
No Missing Codes	Standard and Fast Mode	11			Bits
	High-Speed Mode	10			Bits
Integral Linearity Error	Standard and Fast Mode			±2	LSB[1]
	High-Speed Mode			±4	LSB
Offset Error				±6	LSB
Gain Error				±4	LSB
Noise	Including Internal V_{REF}		70		µVrms
Power-Supply Rejection Ratio			70		dB
SAMPLING DYNAMICS					
Throughput Rate			50		ksps
Channel-to-Channel Isolation	V_{IN} = 2.5Vp-p at 50kHz		100		dB
SWITCH DRIVERS					
On-Resistance					
Y+, X+			5.5		Ω
Y–, X–			7.3		Ω
Drive Current[2]	Duration 100ms			50	mA
REFERENCE OUTPUT					
Internal Reference Voltage		2.45	2.50	2.55	V
Internal Reference Drift			25		ppm/°C
Output Impedance	Internal Reference ON		300		Ω
	Internal Reference OFF		1		GΩ
Quiescent Current	PD1 = 1, PD0 = 0, SDA, SCL High		750		µA
REFERENCE INPUT					
Range		2.0		V_{DD}	V
Resistance	PD1 = PD0 = 0		1		GΩ
BATTERY MONITOR					
Input Voltage Range		0.5		6.0	V
Input Impedance	Sampling Battery		10		kΩ
	Battery Monitor OFF		1		GΩ
Accuracy	External V_{REF} = 2.5V	–2		+2	%
	Internal Reference	–3		+3	%
TEMPERATURE MEASUREMENT					
Temperature Range		–40		+85	°C
Resolution	Differential Method[3]		1.6		°C
	TEMP0[4]		0.3		°C
Accuracy	Differential Method[3]		±2		°C
	TEMP0[4]		±3		°C
DIGITAL INPUT/OUTPUT					
Logic Family			CMOS		
Logic Levels, Except $\overline{PENIRQ}$					
V_{IH}	$\lvert I_{IH} \rvert \le +5\mu A$	$+V_{DD}$ • 0.7		$+V_{DD}$ + 0.3	V
V_{IL}	$\lvert I_{IL} \rvert \le +5\mu A$	–0.3		$+V_{DD}$ • 0.3	V
V_{OH}	I_{OH} = –250µA	$+V_{DD}$ • 0.8			V
V_{OL}	I_{OL} = 250µA			0.4	V
$\overline{PENIRQ}$ V_{OL}	30kΩ Pull-Up			0.4	V
Data Format			Straight Binary		
Input Capacitance	SDA, SCL Lines			10	pF

ELECTRICAL CHARACTERISTICS (Cont.)

At T_A = –40°C to +85°C, $+V_{DD}$ = +2.7V, V_{REF} = 2.5V external voltage, I²C bus frequency = 3.4MHz, 12-bit mode and digital inputs = GND or $+V_{DD}$, unless otherwise noted.

PARAMETER	CONDITIONS	TSC2003I			
		MIN	TYP	MAX	UNITS
POWER-SUPPLY REQUIREMENTS					
$+V_{DD}$	Specified Performance	2.7		3.6	V
	Operating Range	2.5		5.25	V
Quiescent Current	Internal Reference OFF, PD1 = PD0 = 0				
	High-Speed Mode: SCL = 3.4MHz		254	650	µA
	Fast Mode: SCL = 400kHz		95		µA
	Standard Mode: SCL = 100kHz		63		µA
	Internal Reference ON, PD0 = 0		1005		µA
Power-Down Current when Part is Not Addressed	Internal Reference OFF, PD1 = PD0 = 0				
	High-Speed Mode: SCL = 3.4MHz		90		µA
	Fast Mode: SCL = 400kHz		21		µA
	Standard Mode: SCL = 100kHz		4		µA
	PD1 = PD0 = 0, SDA = SCL = $+V_{DD}$			3	µA
Power Dissipation	$+V_{DD}$ = +2.7V			1.8	mW
TEMPERATURE RANGE					
Specified Performance		–40		+85	°C

NOTES: (1) LSB means Least Significant Bit. With V_{REF} equal to +2.5V, one LSB is 610µV. (2) Ensured by design, but not tested. Exceeding 50mA source current may result in device degradation. (3) Difference between TEMP0 and TEMP1 measurement. No calibration necessary. (4) Temperature drift is –2.1mV/°C.

TIMING CHARACTERISTICS

At T_A = –40°C to +85°C, $+V_{DD}$ = +2.7V, unless otherwise noted. All values referred to V_{IHMIN} and V_{ILMAX} levels.

PARAMETER	SYMBOL	CONDITIONS	MIN	MAX	UNITS
SCL Clock Frequency	f_{SCL}	Standard Mode	0	100	kHz
		Fast Mode	0	400	kHz
		High-Speed Mode, C_b = 100pF max	0	3.4	MHz
		High-Speed Mode, C_b = 400pF max	0	1.7	MHz
Bus Free Time Between a STOP and Start Condition	t_{BUF}	Standard Mode	4.7		µs
		Fast Mode	1.3		µs
Hold Time (Repeated) START Condition	$t_{HD;\ STA}$	Standard Mode	4.0		µs
		Fast Mode	600		ns
		High-Speed Mode	160		ns
LOW Period of the SCL Clock	t_{LOW}	Standard Mode	4.7		µs
		Fast Mode	1.3		µs
		High-Speed Mode, C_b = 100pF max	160		ns
		High-Speed Mode, C_b = 400pF max	320		ns
HIGH Period of the SCL Clock	t_{HIGH}	Standard Mode	4.0		µs
		Fast Mode	600		ns
		High-Speed Mode, C_b = 100pF max	60		ns
		High-Speed Mode, C_b = 400pF max	120		ns
Setup Time for a Repeated START Condition	$t_{SU;\ STA}$	Standard Mode	4.7		µs
		Fast Mode	600		ns
		High-Speed Mode	160		ns
Data Setup Time	$t_{SU;\ DAT}$	Standard Mode	250		ns
		Fast Mode	100		ns
		High-Speed Mode	10		ns
Data Hold Time	$t_{HD;\ DAT}$	Standard Mode	0	3.45	µs
		Fast Mode	0	0.9	µs
		High-Speed Mode, C_b = 100pF max	0	70	ns
		High-Speed Mode, C_b = 400pF max	0	150	ns
Rise Time of SCL Signal	t_{rCL}	Standard Mode		1000	ns
		Fast Mode	20 + 0.1C_b	300	ns
		High-Speed Mode, C_b = 100pF max	10	40	ns
		High-Speed Mode, C_b = 400pF max	20	80	ns
Rise Time of SCL Signal After a Repeated START Condition and After an Acknowledge Bit	t_{rCL1}	Standard Mode		1000	ns
		Fast Mode	20 + 0.1C_b	300	ns
		High-Speed Mode, C_b = 100pF max	10	80	ns
		High-Speed Mode, C_b = 400pF max	20	160	ns

TIMING CHARACTERISTICS (Cont.)

At T_A = –40°C to +85°C, $+V_{DD}$ = +2.7V, unless otherwise noted. All values referred to V_{IHMIN} and V_{ILMAX} levels.

PARAMETER	SYMBOL	CONDITIONS	MIN	MAX	UNITS
Fall Time of SCL Signal	t_{rCL}	Standard Mode		300	ns
		Fast Mode	$20 + 0.1C_b$	300	ns
		High-Speed Mode, C_b = 100pF max	10	40	ns
		High-Speed Mode, C_b = 400pF max	20	80	ns
Rise Time of SDA Signal	t_{rDA}	Standard Mode		1000	ns
		Fast Mode	$20 + 0.1C_b$	300	ns
		High-Speed Mode, C_b = 100pF max	10	80	ns
		High-Speed Mode, C_b = 400pF max	20	160	ns
Fall Time of SDA Signal	t_{fDA}	Standard Mode		300	ns
		Fast Mode	$20 + 0.1C_b$	300	ns
		High-Speed Mode, C_b = 100pF max	10	80	ns
		High-Speed Mode, C_b = 400pF max	20	160	ns
Setup Time for STOP Condition	$t_{SU;\ STO}$	Standard Mode	4.0		µs
		Fast Mode	600		ns
		High-Speed Mode	160		ns
Capacitive Load for SDA or SCL Line	C_b	Standard Mode		400	pF
		Fast Mode		400	pF
		High-Speed Mode, SCL = 1.7MHz		400	pF
		High-Speed Mode, SCL = 3.4MHz		100	pF
Pulse Width of Spike Suppressed	t_{SP}	Fast Mode	0	50	ns
		High-Speed Mode	0	10	ns
Noise Margin at the HIGH Level for Each Connected Device (Including Hysteresis)	V_{nH}	Standard Mode Fast Mode High-Speed Mode	$0.2V_{DD}$		V
Noise Margin at LOW Level for Each Connected Device (Including Hysteresis)	V_{nL}	Standard Mode Fast Mode High-Speed Mode	$0.1V_{DD}$		V

TIMING DIAGRAM

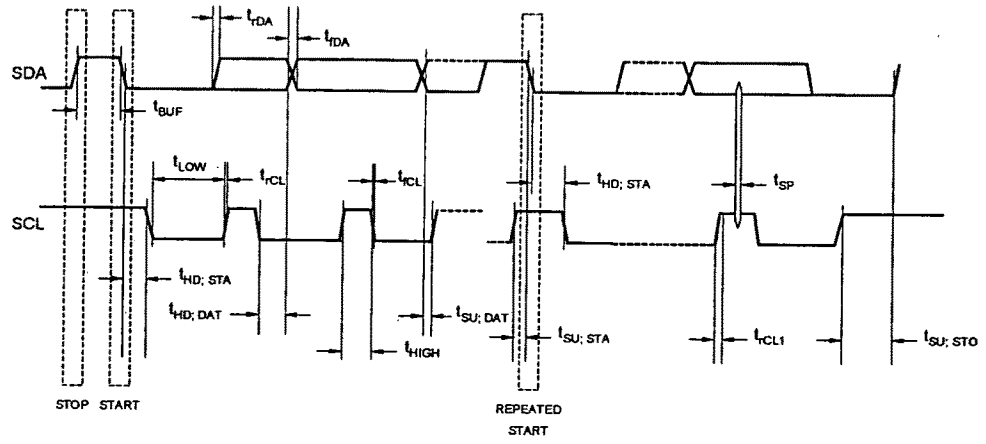

TYPICAL CHARACTERISTICS: +2.7V

At T_A = +25°C, $+V_{DD}$ = +2.7V, V_{REF} = External +2.5V, I²C bus frequency = 3.4MHz, PD1 = PD0 =0, unless otherwise noted.

SUPPLY CURRENT vs TEMPERATURE

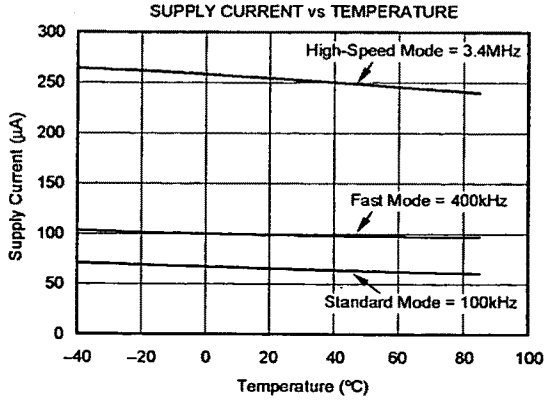

SUPPLY CURRENT vs V_{DD}

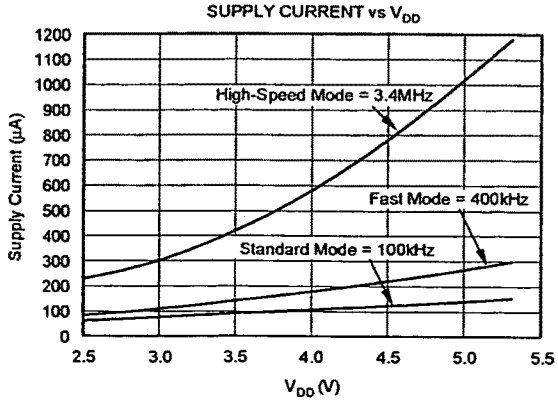

SUPPLY CURRENT vs I²C BUS FREQUENCY

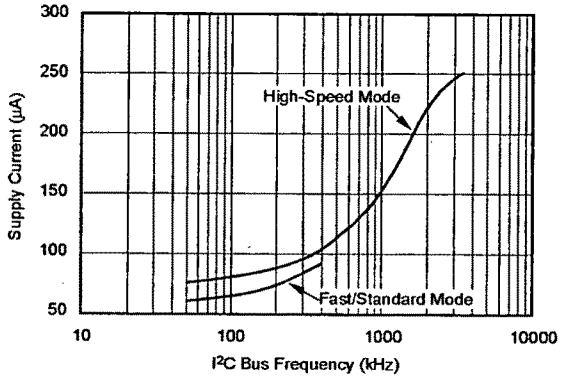

SUPPLY CURRENT (Part Not Addressed) vs V_{DD}

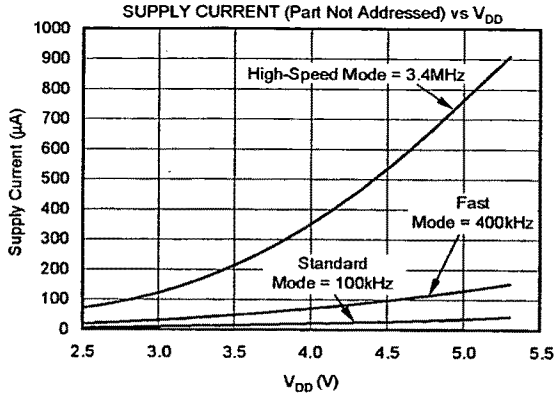

SUPPLY CURRENT (Part Not Addressed) vs TEMPERATURE

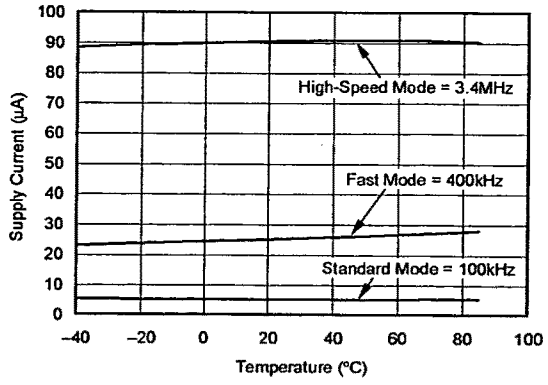

CHANGE IN GAIN vs TEMPERATURE